Reduction in PLANT DEFENSIN 1 expression in Arabidopsis thaliana results in increased resistance to pathogens and zinc toxicity

Nga N T Nguyen, Olivier Lamotte, Mohanad Alsulaiman, Sandrine Ruffel,
Gabriel Krouk, Nathalie Berger, Vincent Demolombe, Claude Nespoulous, Thi
Minh Nguyet Dang, Sébastien Aimé, et al.

▶ To cite this version:

HAL Id: hal-04133593
https://hal.inrae.fr/hal-04133593v2

Submitted on 20 Jun 2023

Reduction in *PLANT DEFENSIN 1* expression in *Arabidopsis thaliana* results in increased resistance to pathogens and zinc toxicity

---

Running Title

PLANT DEFENSIN 1 silencing in Arabidopsis

Nga N. T. **Nguyen**[1], Olivier **Lamotte**[2], Mohanad **Alsulaiman**[1], Sandrine **Ruffel**[1], Gabriel **Krouk**[1], Nathalie **Berger**[1], Vincent **Demolombe**[1], Claude **Nespoulous**[1], Thi Minh Nguyet **Dang**[1], Sébastien **Aimé**[2], Pierre **Berthomieu**[1], Christian **Dubos**[1], David **Wendehenne**[2], Denis **Vile**[3, *], and Françoise **Gosti**[1, 4, *]

* **These authors equally contributed to this work and both agree to serve as co-last authors**

Addresses of the institutions where the work was carried out:

[1] IPSiM, CNRS, INRAE, Institut Agro, Univ. Montpellier, 2, Place P. Viala, F-34 060 Montpellier Cedex 2, France

[2] Agroécologie, CNRS, INRAE, Institut Agro, Université de Bourgogne, Université Bourgogne-Franche Comté, F-21 000 Dijon, France

[3] LEPSE, INRAE, Institut Agro, Univ Montpellier, 2 Place P. Viala, F-34 060 Montpellier Cedex 2, France

email address of each author:

ngocnga080987@gmail.com
olivier.lamotte@inrae.fr
mohanadalsulaiman@gmail.com
sandrine.ruffel@inrae.fr
gkrouk@gmail.com
nathalie.berger@inrae.fr
vincent.demolombe--liozu@inrae.fr
claude.nespoulous@inrae.fr
thi-minh-nguyet.dang@ird.fr
sebastien.aime@inrae.fr
pierre.berthomieu@supagro.fr
christian.dubos@inrae.fr
david.wendehenne@inrae.fr
denis.vile@inrae.fr
francoise.gosti@cnrs.fr

[4] **Correspondence should be addressed to:**
Françoise Gosti
Tel: +33 499 613 084
Email: francoise.gosti@cnrs.fr

Date of Re-submission: April 28th 2023

christian.dubos@inrae.fr

david.wendehenne@inrae.fr

denis.vile@inrae.fr

francoise.gosti@cnrs.fr

⁴ Correspondence should be addressed to:

Françoise Gosti

Tel: +33 499 613 084

Email: francoise.gosti@cnrs.fr

Abstract

Ectopic expression of defensins in plants correlates with their increased capacity to withstand abiotic and biotic stresses. This applies to *Arabidopsis thaliana*, where some of the seven members of the *PLANT DEFENSIN 1* family (*AtPDF1*) are recognised to improve plant responses to necrotrophic pathogens and increase seedling tolerance to excess zinc (Zn). However, few studies have explored the effects of decreased endogenous defensin expression on these stress responses.

Here, we carried out an extensive physiological and biochemical comparative characterisation of i) novel amiRNA lines silenced for the five most similar *AtPDF1*s, and ii) a double null mutant for the two most distant *AtPDF1*s.

Silencing of five *AtPDF1* genes was specifically associated with increased aboveground dry mass production in mature plants under Zn excess conditions, and with increased plant tolerance to different pathogens – one fungus, one oomycete and one bacterium, while the double mutant behaved similarly to the WT.

These unexpected results challenge the current paradigm describing the role of PDFs in the plant response to stresses. Additional roles of plant endogenous defensins are discussed, which open new perspectives for their functions.

Key-words

Highlight

Decreased endogenous AtPDF1 levels are associated with increased tolerance to pathogens and zinc toxicity, while better tolerance to stresses had so far been associated with ectopic *PDF* over-expression.

Introduction

Plants are continuously exposed to simultaneous environmental changes whose intensity and duration interfere with their optimal growth and reproduction. Plant responses to biotic and abiotic stresses rely on different signalling pathways leading to changes at the physiological, molecular and cellular levels (Yamaguchi-Shinozaki & Shinozaki, 2006; Ahuja *et al.*, 2010; Skirycz & Inze, 2010; Osakabe *et al.*, 2014). This results in better adaptation including cross-talk between signalling pathways (Fujita *et al.*, 2006; Rejeb *et al.*, 2014; Pandey *et al.*, 2015; Foyer *et al.*, 2016; Nejat & Mantri, 2017). This fine tuning climaxes when it comes to balancing the trade-off between growth maintenance and the energetic cost of adaptation to abiotic stress and/or biotic defence processes (Denance *et al.*, 2013; Bechtold & Field, 2018; Berens *et al.*, 2019; Chen *et al.*, 2021). Defensin is a generic term encompassing PLANT DEFENSINs (PDFs) and PLANT DEFENSIN-LIKE (DEFLs) peptides which both are integral parts of the plant immune system (Lay & Anderson, 2005; Stotz *et al.*, 2013; Lacerda *et al.*, 2014). Defensins are involved in a wide range of biological activities and physiological processes (Carvalho & Gomes, 2009; Carvalho & Gomes, 2011; Parisi *et al.*, 2019); as such, they are downstream elements of these biotic and abiotic stress-signalling cascades. PDFs and DEFLs are members of the large ANTIMICROBIAL PEPTIDES (AMPs) family (Van der Weerden & Anderson, 2013; Shafee *et al.*, 2016a; Shafee *et al.*, 2017). These molecules have a characteristic three-dimensional folding (three anti-parallel β-strands and one α-helix) stabilised by disulphide bonds (Lehrer, 2004; Yount & Yeaman, 2004; Yount & Yeaman, 2006; Padovan *et al.*, 2010; Gachomo *et al.*, 2012; Shafee *et al.*, 2016b).

The antifungal activity of defensins was first – widely – studied (Lay & Anderson, 2005; De Coninck *et al.*, 2013; Lacerda *et al.*, 2014; Parisi *et al.*, 2019; Sher Khan *et al.*, 2019). Defensins have been described to bind preferentially to lipid II (Wilmes *et al.*, 2011), to the fungal acidic sphingolipids mannosyldiinositol phosphorylceramide [M(IP)2C; (Thevissen *et al.*, 2004)], and the neutral sphingolipids glucosylceramide (GlcCer; Thevissen *et al.*, 2004), to phosphatidic acid (PA; (Sagaram *et al.*, 2013; Kvansakul *et al.*, 2016; Payne *et al.*, 2016) and to phosphatidylinositol 4,5 bis-phosphate [PI(4,5)P2; (Poon *et al.*, 2014; Baxter *et al.*, 2015]]. In addition, the novel *Medicago truncatula* Def5 (MtDef5) bi-domain plant defensin binds to several membrane-resident phospholipids with preference for phosphatidylinositol monophosphates (Islam *et al.*, 2017). Defensin activity also involves production of reactive oxygen species (Aerts *et al.*, 2007; Oyinloye *et al.*, 2015) and induction of fungal cell wall stress (Thevissen *et al.*, 2012). Defensins are also involved in defence against insects by reducing the activity of insect digestive enzymes (Melo *et al.*, 2002; Liu *et al.*, 2006; Pelegrini *et al.*, 2008). Regarding metal abiotic stress, the expression of antifungal *PLANT DEFENSIN 1* (*PDF1*) was first identified as a gain of function in zinc (Zn) tolerance in yeast and in *Arabidopsis thaliana* seedlings (Mirouze *et al.*, 2006; Shahzad *et al.*, 2013; Mith *et al.*, 2015). The constitutive high transcript of *PDF1*s in the metal extremophile *A. halleri* is presently the main feature distinguishing this family from the one present in its close relative and model species *A. thaliana* (Becher *et al.*, 2004; Weber *et al.*, 2004; Talke *et al.*, 2006; van de Mortel & Aarts, 2006; Shahzad *et al.*, 2013). Recent genetic studies have identified a *DEFL – CADMIUM ACCUMULATION IN LEAVES 1 (CAL1*) – as a driver of cadmium (Cd) efflux and allocation in rice through chelation and transport activities (Luo *et al.*, 2018; Luo *et al.*, 2020), together with the close relative dual-function DEFENSIN 8 which mediates phloem cadmium unloading and accumulation in rice grains (Gu *et al.*, 2022). In *A. thaliana*, *AtPDF2.5* and *AtPDF2.6* are suggested to be involved in Cd tolerance (Luo, J-S *et al.*, 2019; Luo, JS *et al.*, 2019). *AtPDF2.1* is proposed to modulate the ammonium metabolism by

regulating glutamine synthase activity (Yao *et al.*, 2019) whereas the antifungal AtPDF2.3 blocks potassium channels (Vriens *et al.*, 2016). In addition, *AtPDF1.5* is probably involved in plant adaptation to low nitrogen levels and Cd stress (Wu *et al.*, 2021).

All these properties highlight that PDF and DEFL peptides are endowed with the remarkable protein promiscuity activity, in which multiple functions are associated with a single peptide structure (Aharoni *et al.*, 2005; Nobeli *et al.*, 2009; Franco, 2011), but the process still remains to be deciphered at the molecular level. On the one hand, studies in various species have highlighted that ectopic expression of defensins correlates with an increased capacity to withstand stresses (Terras *et al.*, 1995; Gao *et al.*, 2000; Dos Santos *et al.*, 2010; Kaur, J *et al.*, 2011; Sagaram *et al.*, 2012; de Souza Candido *et al.*, 2014; Gaspar *et al.*, 2014; Wei *et al.*, 2020). On the other hand, inactivation of single endogenous defensin genes has rarely been tested and has not always resulted in altered plant phenotypes in response to pathogens (Stotz *et al.*, 2009; De Coninck *et al.*, 2010). The existence of functional redundancy among defensins was hypothesized following the discovery of more than 300 DEFL peptides, first in *A. thaliana* and then in other plant genomes (Silverstein *et al.*, 2005; Silverstein *et al.*, 2007; Tesfaye *et al.*, 2013; Van der Weerden & Anderson, 2013). Superimposed on this framework, hardly any study have investigated whether decreased endogenous defensin expression would affect different functions in the same way, reflecting the existence of some specificity and/or cross-talk of the defensin signalling response to biotic and abiotic stresses.

Faced with this bottleneck, in response to biotic and abiotic stresses, we studied the effect of simultaneous silencing expression of the five most similar *PDF1* members (*i.e*. *AtPDF1.1*, *1.2a*, *1.2b*, *1.2c*, and *1.3*) out of the seven composing this multigenic family in *A. thaliana*. The *AtPDF1*s members have all been described to provide better Zn tolerance when expressed in yeast (Mirouze *et al.*, 2006; Shahzad *et al.*, 2013; Mith *et al.*, 2015). In seedlings, *AtPDF1* transcripts are not responsive to Zn (Nguyen *et al.*, 2014), but their syntenic orthologues are all highly accumulated in the hyper-accumulating and metal-tolerant species *A. halleri* (Weber *et al.*, 2004; Talke *et al.*, 2006; Shahzad *et al.*, 2013) and *Noccaea caerulescens* [formerly *Thlaspi caerulescens*; (Hammond *et al.*, 2006; van de Mortel & Aarts, 2006; van de Mortel *et al.*, 2006)]. Five of them (*AtPDF1.1*, *1.2a*, *1.2b*, *1.2c* and *1.3*) have been positively tested in the plant response to pathogens, either *in vitro* (Terras *et al.*, 1993; Sels *et al.*, 2007), or in transgenic plants (Zimmerli *et al.*, 2004; De Coninck *et al.*, 2010; Hiruma & Takano, 2011; Hsiao *et al.*, 2017). The variation of *AtPDF1.1* expression has no or little effect upon plant infection with necrotrophic *B. cinerea* or with the non-host pathogen *Cercospora beticola*, respectively (De Coninck *et al.*, 2010), whereas this gene has been proposed to mediate defence *via* an iron-withholding defence system in response to the necrotrophic bacterium *Pectobacterium carotovorum* (Hsiao *et al.*, 2017). *AtPDF1.2a* is a marker of the jasmonic acid response (Yan *et al.*, 2009; Pieterse *et al.*, 2012), and *AtPDF1.2a, 1.2c*, and *1.3* transcripts have been described for their similar positive response to non-host pathogens (Hiruma & Takano, 2011). The mature peptides encoded by *AtPDF1.2a*, *1.2b* and *1.2c* are identical, and they differ from *AtPDF1.3* by only one amino acid (Sels *et al.*, 2008; De Coninck *et al.*, 2013) This, together with the similar tissue localisation of the expression of several of these genes (Sels *et al.*, 2008), suggest the existence of a potential functional redundancy between these genes, as already mentioned (De Coninck *et al.*, 2013).

To study the effects of decrease expression of the *AtPDF1* endogenous genes, we associated genetic approaches using T-DNA null mutants and amiRNA plants, and carried out an extensive

characterisation of these lines as compared to the wild type (WT) in response to different pathogens and metal excess. Given the abundant literature describing that defensin over-expression improves the plant response to biotic and/or abiotic stresses (Gao *et al.*, 2000; Carvalho & Gomes, 2011; Kaur, J *et al.*, 2011; Gaspar *et al.*, 2014), the null hypothesis was that decreased endogenous *AtPDF1* transcript would result in a plant phenotype more sensitive to stresses. The results presented here do not support this assumption. Instead, the transgenic lines whose *AtPDF1* expression was decreased were more tolerant to different pathogens and displayed specific increased dry mass in response to Zn excess. These unexpected and puzzling results modify the defensin-plant stress response paradigm in the same way, i.e., an increased tolerance to both biotic and abiotic stresses. Several alternative hypotheses on additional roles of endogenous plant defensins are discussed, and will call for further testing.

Materials and Methods

Plant material and growth conditions

All *A.thaliana* lines were in the Columbia-0 (Col-0) accession background. Seeds of wild type plants (WT, N60000) and T-DNA insertion lines *Atpdf1.4* (GK-311B04) and *Atpdf1.5* (SALK_151733) were purchased from the Nottingham Arabidopsis Stock Centre (http://arabidopsis.info/). The transgenic lines, which express *AhPDF1.1b* under the 35S promoter, are described in Mirouze *el al* (2006). The homozygous single *Atpdf1.4* and *Atpdf1.5* mutants were checked by polymerase chain reaction (PCR) (Supplementary Table S1; Supplementary Fig. S1) and characterised by real-time quantitative PCR (RT-qPCR) for the absence of corresponding *AtPDF1* transcripts using specific oligonucleotides (Nguyen *et al.*, 2014) to ensure that these mutant lines were null mutants (Supplementary Table S2). The double null *Atpdf1.4-Atpdf1.5* mutant was identified by PCR (Supplementary Table S1) in the F2 generation produced from a genetic cross between single *Atpdf1.4* and *Atpdf1.5* mutants. The *lacs2-3* mutant affected in *LONG-CHAIN ACYL-COA SYNTHETASE 2* is described in (Bessire *et al.*, 2007). In order to make crosses, propagate seeds or collect plant materials, *A. thaliana* plants were cultivated at 22°C in a glasshouse in individual small pots containing compost (Neuhaus N2). When the intensity of natural light was less than 130 µmol m^{-2} s^{-1}, artificial light (220 µmol m^{-2} s^{-1}) was supplied up to 16 h *per* day.

In vitro cultivation experiments were conducted under axenic conditions in a growth chamber at 21.5°C under a 16-h daily light cycle and 130 µmol m^{-2} s^{-1} light intensity. Surface-sterilised seeds were germinated on standard medium containing Murashige and Skoog inorganic salts (Murashige & Skoog, 1962) at half concentration, with 1% (w/v) sucrose, 0.8% (w/v) agar and 2.5 mM (2-[N-morpholino] ethanesulphonic acid) - KOH at pH 5.7. Kanamycin (Km) was added at a final concentration of 50 mg l^{-1} to screen transgenic *A. thaliana* lines. Phenotypic analyses of soil-grown plants were performed on plants grown in individual pots containing compost (Neuhaus N2) and placed in standard growth chambers with an 8-h-light photoperiod, 165 to 170 mmol m^{-2} s^{-1} photosynthetic photon flux density, 21-23°C/17-23°C day/night temperatures, respectively, and 70% air relative humidity. Seeds were sown at the soil surface, and plants were irrigated manually to reach 0.35 g of water g^{-1} dry soil or watered by sub-irrigation every four to five days. For phenotypic analysis of hydroponically grown plants, plants were cultivated in controlled growth chambers under an 8-h daily light cycle under 165 µmol m^{-2} s^{-1} light intensity, and 20/23°C night/day temperature. Seeds were first germinated in tubes containing sterilised solid medium composed of Murashige and Skoog inorganic salts at half concentration (Murashige & Skoog, 1962), with 0.8% (w/v) agar and 2.5

mM (2-[N-morpholino] ethanesulphonic acid) - KOH at pH 5.7. At the five-to-six-leaf stage, the plantlets were transferred to hydroponic basins containing nutrient solution composed of 3 mM KNO_3, 2 mM $Ca(NO_3)^2$-$4H_2O$, 1 mM $NH_4H_2PO_4$, 0.5 mM $MgSO_4$-$7H_2O$, 1 μM KCl, 25 μM H_3BO_3, 2 μM $ZnSO_4$, 2 μM $MnSO_4$, 0.1 μM $CuSO_4$-$5H_2O$, 0.1 μM $(NH_4)6Mo_7O_{24}$, 20 μM Fe(Na)EDTA and 2.5 mM (2-[N-morpholino] ethanesulphonic acid) - KOH at pH 5.7, and renewed every four days. For phenotypic analysis of cuticle permeability and susceptibility to pathogens, plants were grown on soil pellets (Jiffy-7) under cool daylight fluorescent tubes (OSRAM) with a 10-h daily light cycle under 120 μmol m^{-2} s^{-1} light intensity, and 18/20°C night/day temperature.

Generation of amiRNA lines targeting a decrease of *AtPDF1* transcript accumulation

Plasmid pBSK-RS300 (Schwab *et al.*, 2006) harbouring the miR319a precursor was used to engineer amiRNAs targeting transcript decreases of all five *AtPDF11.1*, *1.2a*, *1.2b*, *1.2c*, and *1.3* simultaneously. Three amiRNA sequences named amiRNA-C1, amiRNA-C2 and amiRNA-C3 (Supplementary Table S3) were automatically designed *via* the Micro RNA Designer website: http://wmd3.weigelworld.org/cgi-bin/webapp.cgi (Schwab *et al.*, 2005; Schwab *et al.*, 2006) and validated and/or improved manually following a set of crucial requirements (Ossowski *et al.*, 2008). No off-target mutation was identified *in silico* when the three 21-bp oligonucleotides were probed with the Araport11genes 201606 cDNA database in the Micro RNA Designer website (http://wmd3.weigelworld.org/cgi-bin/webapp.cgi?page=TargetSearch;project=stdwmd), or when they were blasted against the NCBI database with the *A. thaliana* Reference RNA sequences (refseq_rna). In both tests, only the five targeted *AtPDF1* sequences were highlighted with the highest e-value (between 0.007 and 0.11). The amiRNA construct and plasmid cloning were performed according to (Schwab *et al.*, 2006). A functional stem-loop structure was regenerated by combining the PCR products obtained using the specific *AtPDF1* primer pairs in a single overlapping PCR with primers A and B bordering the miR319a stem-loop structure in plasmid pBSK-RS300 (Supplementary Table S3). The amiRNA constructs were cloned between the 35S promoter and Terminator Nos using the *Xho*I and *Xba*I restriction sites present in pKYLX71, a designed pBluescriptII-based plasmid [Stratagene®, Schardl *et al.*, 1987)]. The expression cassette containing the amiRNA loop was further cloned in the pGreen 0029 binary vector (Hellens *et al.*, 2000) in-between the *Xma*I and *Kpn*I restriction sites to form the final recombinant vector pGrenn029-35S-amiRNA-C1 or -C2 or -C3. These final vectors were then transformed into *Agrobacterium tumefaciens* strain GV3103 (pMP90; Koncz & Schell, 1986). Positive bacterial transformant for each of the final recombinant vector were used to transform *A. thaliana* plants by floral dipping (Clough & Bent, 1998). Seeds resistant to Km (Km^R) obtained from primary transformed plants were selected, and their progeny was screened for a one-locus mendelian segregation of the Km^R character. A total of 25 independent homozygous transgenic amiRNA lines were obtained (eight to nine *per* construct, listed in Supplementary Dataset S1). From now on, these homogeneous transgenic amiRNA lines named amiRNA-C1, amiRNA-C2 and amiRNA-C3 thereafter, will be generally referred to "amiRNA lines" or "amiRNA plants".

Quantitative Real Time PCR (qRT-PCR)

Total RNA was extracted from the shoots of seedlings grown *in vitro* using the RNeasy kit (Qiagen, 74904). For plants grown in soil and submitted to pathogenesis tests, RNAs were extracted according to (Mallory *et al.*, 2001). Transcript was quantified by qRT-PCR. cDNA synthesis and qRT-PCR were essentially performed as previously described (Shahzad *et al.*, 2013; Nguyen *et al.*, 2014). For *AtPDF1*s, the primer list, location in the cDNA sequences, amplification efficiency and specificity were already described (Nguyen *et al.*, 2014). PCRs were performed on cDNA samples in triplicate, and given the high variability range of *AtPDF1* transcript (Supplementary Fig. S2B; Supplementary Table S4), threshold cycles (Ct) were considered up to 40 cycles. Above this value, transcripts were considered as non-detected (ND), as indicated by the qPCR system. Transcript was expressed with respect to three reference genes chosen as internal controls for their strong expression stability under different developmental stages, abiotic and biotic treatments (Czechowski *et al.*, 2005; Remans *et al.*, 2008; Rymaszewski *et al.*, 2017; Veillet *et al.*, 2017; Li *et al.*, 2020). For the transcript studied in seedlings of different genotypes in Fig. 1B and Supplementary Fig. S5) we used: *ACTIN* [*ACT2*, AT3G18780 and *ACT8*, AT1G49240] already described by (Shahzad *et al.*, 2010; Shahzad *et al.*, 2013; Nguyen *et al.*, 2014), *YELLOW-LEAF-SPECIFIC GENE 8* (*YSL8*, AT5G08290, 5'-TTACTGTTTCGGTTGTTCTCCATTT -3' and 5'- CACTGAATCATGTTCGAAGCAAGT -3'), and *ELONGATION FACTOR 1 ALPHA* (*EF1alpha*, AT5G60390, 5'- TGAGCACGCTCTTCTTGCTTTCA -3' and 5'-GGTGGTGGCATCCATCTTGTTACA -3') as reference genes. For the transcript studied in plants following *B. cinerea* treatments (Fig. 2C and Supplementary Fig. S9) we used: *ACTIN* (*ACT2* and *ACT8*), *YSL8* and *expressed gene* in AT4G26410 (5'- GAGCTGAAGTGGCTTCCATGAC-3' and 5'-GGTCCGACATACCCATGATCC-3') as reference genes. The *AtPDF1* transcript accumulations calculated independently with respect to each of the three reference genes were significantly and highly correlated ($P < 0.001$; Supplementary Fig. S3 and Supplementary Fig. S4) demonstrating the high consistency of these values among these reference genes.

Zinc (Zn) and other metal treatment of mature plants

For plants grown in soil, Zn treatment was applied by daily manual watering with solutions containing different $ZnSO_4$ concentrations to maintain the soil water content at 0.35 g water g^{-1} dry soil, or by sub-irrigation every four to five days with solutions containing different $ZnSO_4$ concentrations. For hydroponic grown plants, the treatment was applied by adding and renewing solutions containing different $ZnSO_4$, $CoCl_2$ or $NiCl_2$ concentrations every four days.

Biochemical measurements

Zn, iron and manganese content measurement: whole rosettes of plants grown hydroponically or in soil were harvested and rinsed thoroughly three times with Milli-Q® water at room temperature for a few minutes. All materials were desiccated at 80°C for 72 hours and ground to powder. Fifteen- to 20-mg subsamples were homogenised with 750 μl of 65% (w/w) HNO_3 and 250 μl of 30% (w/w) H_2O_2 and mineralised in a microwave oven using a temperature step gradient (100, 180, 145 and 75°C) for 50 min and holding for 30 min. After five-fold dilution with Milli-Q® water, 1 ml from each sample was diluted again five-fold in 10% (w/w) HNO_3 and analysed for its Zn, iron and manganese content

by inductively coupled plasma mass spectrometry (MP-AES, Agilent®) and compared with reference standard elements.

Shoot anthocyanins content: anthocyanins were extracted and analysed according to (Nakata & Ohme-Takagi, 2014). The shoot fresh weight (FW) was measured directly after harvesting, and the shoots were frozen in liquid nitrogen for grinding. Extraction buffer (45% methanol, 5% acetic acid) was added at a ratio of 15 ml *per* g FW. Samples were centrifuged twice at 12,000 x g at room temperature for five minutes, and absorbance (A) was read at 530 and 657 nm on the supernatant. The anthocyanin content was calculated as (A530 g FW^{-1}):[A530 - (0.25 x A657)] according to (Nakata & Ohme-Takagi, 2014).

Liquid Chromatography Coupled with Mass Spectrometry (LC-MS/MS) Analysis

Proteins, from pools of 3 rosettes from 6-weeks-old plants, pools of *ca.* 10 of 21-days-old seedlings aerial parts and *ca.* 10 mg of dry seeds, were extracted with 6M urea, 50mM Tris-HCl, EDTA-free protease inhibitor cocktail. In the case of seed protein extraction 1% PolyVinylPyrrolidone (PVP) was added. Protein concentration was measured (Bradford, 1976) using Pierce™ Detergent Compatible Bradford Assay Kit (ThermoScientific). For each sample 20μg of extracted proteins were loaded on a 15% acrylamide SDS-PAGE gel and subjected to a 1h migration at 120V. A band corresponding to a protein migration of around 10kDa was cut for each loaded lane and treated for trypsin digestion as described in (Berger *et al.*, 2020) before injection in an Orbitrap Exploris™ 240 mass spectrometer for mass spectrometry analysis.

Mass spectrometric raw data were analyzed in the MaxQuant environment [(Cox & Mann, 2008); v.2.0.3.0] and Andromeda software was employed for database searching (Cox *et al.*, 2011). The MS/MS data were matched against the Araport11_genes_20210122 database. For protein identification and quantification, cysteine carbamidomethylation was set up as fixed modification and oxidation of methionine as a variable modification. At least one peptide is necessary for protein identification and quantification with a score at least equal to 20 for unmodified peptides and a score of 40 for modified peptides. Up to two missed cleavages was allowed for protease digestion. For other characteristics, MaxQuant default parameters were used. The normalization was performed as described in (Berger *et al.*, 2022). Following the quantification and normalization step, proteins were considered as quantifiable only if they were present in at least two biological replicates. The normal distribution of the log-transformed data was assessed before statistical treatment (one-way ANOVA followed by post hoc Tukey test, *P*<0.05).

Plant trait measurements

Aboveground dry mass was determined after drying plant material at 80°C for three days. Specific leaf area (SLA; mm^2 mg^{-1}) was calculated using one fully expanded leaf *per* plant, whose area was determined by image analysis (Schneider *et al.*, 2012). The dry weight of each leaf was determined after drying at 80°C for 72 h. Flowering time was monitored on plants grown from seeds in soil under short days. Plants were checked visually every day for flowering bud appearance. The date of flowering bud appearance was monitored together with the concomitant total number of leaves.

Pathogenicity test

Botrytis. cinerea strain BMM (Zimmerli *et al.*, 2001) was cultured on V8-agar medium (50% of V8® Vegetable Juice, Campbells (v/v), 37 mM KH_2PO_4, agar 15 g l^{-1}, pH 6) at 22 °C in the dark for seven to 10 days. Spores were harvested using sterile water and filtered through sterile gauze to remove hyphae. Concentrated spore solutions (>1 10^8 spores ml^{-1}) can be kept at 4°C for 10 days. A spore solution (5 10^4 spores ml^{-1}) was prepared in potato dextrose broth (PDB, Difco) at 6 g l^{-1} for inoculation. Six-µl droplets of spore solution were deposited on four leaves of four-week-old plants, and lesion diameters were measured using a caliper after five days. Seven to eight plants *per* genotype were used in each biological replicate. During infection, plants were placed in high humidity in covered trays. For qRT-PCR analysis, four-week-old plants were sprayed with a spore solution (2 10^5 spores ml^{-1}) prepared in PDB 6 g l^{-1} or with PDB alone as a mock control and kept in high humidity in covered trays. Samples were harvested at the indicated time point and frozen in liquid nitrogen.

Hyaloperonospora. arabidopsidis isolate NOCO (Slusarenko & Schlaich, 2003) was maintained every week by spraying a solution of spores (5 10^4 spores ml^{-1} sterile distilled water) on 10-day-old *A. thaliana* Col-0 seedlings. For the pathogenicity test, seven three-week-old plants were inoculated by spraying a solution of spores (5 10^4 spores ml^{-1} sterile distilled water) and placed in high humidity in a tray closed with a transparent lid. The next day, the tray was partially opened. Six days *post* inoculation, the lid was sprayed with water and the tray was closed to induce sporulation, which was analysed one day later by collecting and pooling four leaves *per* plant in a laboratory glass pillbox and weighing them. Ten ml of sterile dH_2O were added, and the leaves were gently shaken using a vortex for four min to harvest *H. arabidopsidis* spores. After filtration using a small stainless-steel metal sieve, spores were counted using a Malassez cell.

Pseudomonas. synringae pv *maculicola ES4326* (Katagiri *et al.*, 2002) growth was conducted at 28°C in media containing 50 µg ml^{-1} rifampicin. A bacterial glycerol stock was plated onto King's B agar plate (20 g l^{-1} peptone special (Millipore), 1% glycerol (v/v), 11 mM KH_2PO_4, 6 mM $MgSO_4$-$7H_2O$, 15 g l^{-1} agar, pH 7.2). After 2 days of growth, a single bacterial colony was grown overnight in King's B liquid medium under shaking. Fifty µl of this culture medium were added to 50 ml of liquid KB medium and incubated overnight under shaking to reach an OD_{600nm} of 0.2. After centrifugation (3,500 rpm, 15 min), each bacterial pellet was resuspended in 10 mM $MgCl_2$. Serial dilutions in 10 mM $MgCl_2$ were made to reach an OD_{600nm} of 0.002 (10^6 bacteria ml^{-1}). For each genotype, three leaves of four-five-week-old plants were infiltrated with this bacterial solution using a 1-ml needleless syringe. The plants were placed in a tray closed with a transparent lid in a high-humidity atmosphere. After 24h, the lid was removed. After 48 h, 7-mm diameter leaf disks were harvested in each infiltrated leaf for each genotype, ground with a mortar and pestle and resuspended in 10 ml of 10 mM $MgCl_2$ to extract the bacteria. One hundred and fifty µl of 10-fold dilutions (10^{-2} to 10^{-5}) were plated onto King's B agar plates and incubated at 28°C. Colony-forming units were counted after two days.

Cuticle permeability assay

Cuticle permeability was evaluated using the toluidine blue test as described by (Bessire *et al.*, 2007) and (L'Haridon *et al.*, 2011), with slight modifications. Six-µl droplets of 0.1% toluidine blue dissolved in water (m v^{-1}) were placed on the leaf surface. The plants were kept in high humidity in covered

trays overnight. The leaves were washed gently with distilled water to remove excess toluidine blue solution, and data were acquired with photographs of the leaves.

Statistical analyses

All results from physiological and biochemical analyses were performed in R programming environment (RCoreTeam, 2020). For each treatment and genotype, the transcript of the five *AtPDF1*s were compared based on mean and bootstrapped 95% confidence intervals (CIs) computed using the Hmisc package. Correlations between relative expression were calculated for each reference gene independently and were tested as highly significant using Pearson's correlation coefficients ($P < 0.001$, Supplementary Fig. S3 and S4). Hence, the relative expression levels of the transcripts were calculated using the geometric mean of three reference genes (Vandesompele *et al.*, 2002; Andersen *et al.*, 2004). Fold changes of transcript were calculated as the ratio of transcript relative to the three reference genes or ACTIN only in transgenic lines and in WT (i.e. $REL_{transgenic\ line}$ / REL_{WT}). In each experiment, differences in lesion diameter between genotypes were compared following Dunnett's multiple comparison test using the WT as a baseline. Differences in the changes in dry weight (% of the control) in response to Zn treatment between genotypes were tested using simultaneous 95% CI for ratios of linear combinations in a one-way ANOVA model using the *sci.ratio* function in the *mratios* package. Differences in leaf Zn content between genotypes were tested by a non-parametric Kruskal-Wallis test. Relationships between harvest time and anthocyanin content were tested using linear regression analysis. All experimental settings, data acquisitions and biological replicates are described in Supplementary Dataset S1, and all raw data are available in Supplementary Dataset S2 and online (https://doi.org/10.15454/AXY7FV). Proteomic data are available via ProteomeXchange with identifier PXD037695.

Results

AtPDF1s transcript and protein accumulation is decreased in amiRNA lines

The *AtPDF1*s family is composed of seven members grouped in three different clades and one of which is gathering five most similar members [(Shahzad *et al.*, 2013) and Supplementary Fig. S2A]. The different *AtPDF1*s accumulate at different levels [(Shahzad *et al.*, 2013; Nguyen *et al.*, 2014), Supplementary Fig. S2B, Supplementary Table S4], and have different plant tissue localisations (Supplementary Fig. S2C). These disparities also occurs at the protein level where, specific peptides detection by mass spectrometry for the five most similar AtPDF1 proteins targeted by our amiRNA approach can vary according to tissue [(Wang *et al.*, 2015; Mergner *et al.*, 2020); summarized in Supplementary Table S5 and S6]. In addition, protein similarity impairs reliable individual specific identification (Fig. 1C). Given the existence of two tandem duplicates separated by only a few kb – [*i.e*. *AtPDF1.2a*, *1.2c* and *AtPDF1.2b*, *1.3* , (Shahzad *et al.*, 2013), Supplementary Fig. S2D)], this makes it difficult to knock-down the whole *AtPDF1*s family by combining multiple crosses of single mutants. Therefore, we designed three independent amiRNA sequences (Supplementary Table S3) targeting different positions in the five most similar *PDF1*s – *AtPDF1.1*, *1.2a*, *1.2c*, *1.2b* and *1.3* – to decrease their respective *AtPDF1* transcript in plants (Fig. 1A). Twenty-five independent homozygous

amiRNA lines expressing one of these different constructs were obtained (listed in Supplementary Dataset S1).

Quantification of *AtPDF1* transcript in seedlings of each independent amiRNA homozygous line (Fig. 1B, Supplementary Fig. S5) showed that in amiRNA lines, *AtPDF1.3* and *AtPDF1.2a* transcripts significantly decreased by fold changes of 0.0966 and 0.0244 relative to the WT, respectively ($P <$ 0.001) while *AtPDF1.1* transcript was detected in the WT but was not detected in the amiRNA seedlings. Moreover, *AtPDF1.2b* and *AtPDF1.2c* were not detected in any WT or amiRNA seedling. As for non-targeted transcripts (*i.e. AtPDF1.4* and *AtPDF1.5*), no significant decrease, or only a marginal one (0.906 for *AtPDF1.4* and 0.404 for *AtPDF1.5*) was detected in the amiRNA lines relatively to the WT. Overall, for each detected *AtPDF1* transcript, no significant difference was observed among amiRNA lines expressing one construct or the other, and transcript decrease in amiRNA lines as compared to the WT was validated statistically.

When performed in over-expressing transgenic plants, detection of higher defensin protein levels relied on specific antibodies [western-blotting or ELISA assay; only to cite a few: (Gao *et al.*, 2000; Kaur *et al.*, 2012; Gaspar *et al.*, 2014)] or antibodies against tagged-defensin fusion. Still comparative analysis of endogenous expressed defensins proteins is rare (Kaur, P *et al.*, 2011). Since no commercial antibodies are available in *A. thaliana*, endogenous AtPDF1s protein quantification relied on proteomic approaches which seems biased by AtPDF1 high similarity and/or low abundance (Fig.1C; Supplementary Table S5 and S6). We performed mass spectrometry analysis on a 10 kDa fraction of each of the different samples from WT, amiRNA-C2 and amiRNA-C3 genotypes No peptide was detected for AtPDF1.4 and AtPDF1.5 (ProteomeXchange with identifier PXD037695). Among the remaining five AtPDF1, although no peptide was detected in the rosette leaves of WT and amiRNA lines, analysis of aerial tissues from seedling reveals a statistical higher peptide detection in WT as compared to both amiRNA-C2 and amiRNA-C3 genotypes for AtPDF1.2a and/or 1.2b and/or 1.2c and/or 1.3 which were even stronger in samples from dry seeds (Fig. 1D, Supplementary Fig. S6 and Supplementary Table S5). Apart from PDF1, additional specific peptides detected some others PDFs or DEFLs as listed in (Silverstein *et al.*, 2005), either in seeds and / or seedlings, but none of them were significantly accumulated differentially in the amiRNA lines compared to WT (Supplementary Table S7).

Overall, the *AtPDF1*-amiRNA approach used in this study is associated with a decrease at the mRNA and protein level of the targeted *AtPDF1* genes. From then on, we performed further phenotypic and molecular analyses on representative amiRNA lines for at least two amiRNA constructs (Supplementary Dataset S1).

The amiRNA plant lines show pleiotropic phenotypes

Upon aging, we first observed that all amiRNA plants flowered earlier and produced fewer leaves than the WT (Supplementary Fig. S7A-B). The leaves of amiRNA plants were also a lighter green than those of the WT (Supplementary Fig. S7C), and appeared larger and thinner. The results of specific leaf area (SLA) quantification (ratio of leaf area to leaf dry mass) were in accordance with these observations: the SLA of amiRNA lines tended to be higher than the SLA of the WT (Supplementary Fig. S7D).

Overall, the amiRNA lines produced using the three different amiRNA constructs exhibited significant differences in development, growth and leaf morphological trait values as compared to the WT, and only marginal differences were observed among the amiRNA lines harbouring the different amiRNA constructs.

Tolerance to different pathogens is increased in amiRNA lines

We investigated the responses of WT plants and amiRNA lines to infection by different micro-organisms: the fungus *B. cinerea* strain BMM which induces necrotic lesions on *A. thaliana* ecotype Col-0 (Zimmerli *et al.*, 2001), the oomycete *H. arabidopsidis* NOCO2 which is virulent on Col-0 plants (Slusarenko & Schlaich, 2003), and the bacterial pathogen *P. syringae* pv *maculicola* ES4326 (Katagiri *et al.*, 2002). Following inoculation with *B. cinerea*, all amiRNA lines exhibited visually less lesion than the WT (Fig. 2A), and similar observation was also made following *H. arabidopsis* and *P. synringae* pv *maculicola* inoculation (Fig. 3A and Fig. 3C, respectively). Lesion sizes measured after *B. cinerea* infection were significantly smaller on amiRNA plants than in WT (Fig. 2B), and *H. arabidopsidis* sporulation was significantly lower on amiRNA plants that in WT plants (Fig. 3B). Regarding *P. synringae* pv *maculicola,* bacterial counts were significantly lower in amiRNA lines in comparison to WT plants (Fig. 3D). This general decrease in pathogen sensitivity was specific to the amiRNA lines. It was not observed in the double *Atpdf1.4-Atpdf1.5* mutant (Supplementary Fig. S8), which behaved like the WT plants whatever the pathogen tested.

Following *B. cinerea* infection, all *AtPDF1.1, 2a*, *1.2b*, *1.2c* and *1.3* transcripts were detected in mock and treated WT plants whereas *AtPDF1.5* transcripts were not (Fig. 2C, Supplementary Fig. S9). Upon botrytis-infection of WT plants, transcript of *AtPDF1.1, 2a*, *1.2b*, *1.2c* and *1.3* increased (Fig. 2C, Supplementary Fig. S9). The fold change of *AtPDF1s* detected in the amiRNA lines as compared to the control WT plants ranged from 18.6 to 0.06. Changes in transcript observed in the infected amiRNA lines as compared to the mock treatment for *AtPDF1.1, 1.2a*, *1.2b, 1.3*, and *1.4* (fold changes of 1.13, 3.95, 2.49, 0.03, 0.89 and 0.80, respectively) were not significant. Moreover, their respective transcript levels never reached that of the infected WT plants: it was around two orders of magnitude lower [fold changes of 0.028, 0.13, 0.0023, 0.11, for *AtPDF1.2a*, *1.2b*, *1.2c* and *AtPDF1.3,* respectively, and of 0.55 and 1.59 but not significant (P = 0.56 and 0.74) for *AtPDF1.1* and *1.4*, respectively (Fig. 2C, Supplementary Fig. S9). Finally, whatever the mock treatment or infection conditions, *AtPDF1.2c* was barely detected in the amiRNA lines (n = 5 out of 30 samples), and *AtPDF1.5* was not detected as observed for WT (Fig. 2C, Supplementary Fig. S9). Overall, these results show that amiRNA plants are more tolerant than WT plants to infection by different pathogens, even in the presence of decreased *AtPDF1*.

The amiRNA plants increase their aboveground dry mass in response to Zn excess without modifying their total leaf Zn content

Zn tolerance gain of function conferred by defensins has been evidenced in transgenic *A. thaliana* expressing *A. halleri PDF1.1b* under the 35S promoter (OE *AhPDF1.1b*). The dry mass of these transgenic seedlings germinated on Zn excess increases as compared to the WT (Mirouze *et al.*, 2006). When applied to all independent amiRNA seedling lines, this germination test under Zn exposure highlighted a significant and specific decrease in shoot dry mass as compared to the WT

and the double *Atpdf1.4-Atpdf1.5* mutant (Mirouze *et al.*, 2006), which behaved similarly (Supplementary Fig. S10A-B). Yet, when mature amiRNA plants were submitted to Zn excess (whether in soil or hydroponics), their aerial dry mass increased as compared to the WT (Fig. 4A-B). This dry mass increase was not significantly detected in *AhPDF1*-over-expressing lines (Supplementary Fig. S10C), or in the double null *Atpdf1.4-Atpdf1.5* mutant (Supplementary Fig. S10D), nor was it detected when amiRNA lines were exposed to other metals such as cobalt (Co), nickel (Ni) or cadmium (Cd) (Supplementary Fig. S11). Contrasted Zn accumulation in the tissues of plants from different genotypes might explain this surprising observation. In all growth conditions, the total Zn content of plant aerial parts specifically increased following Zn addition in the medium (Fig. 4C) as compared to the (Fe) and manganese (Mn) contents (Supplementary Fig. S12), but no significant difference in Zn, Fe or Mn contents was observed between the WT and amiRNA lines (Fig. 4C and Supplementary Fig. S12). Overall, the aboveground dry mass of mature amiRNA plants specifically increased under Zn excess exposure, but no link was established with the Zn content.

In the amiRNA plants, tolerance to Zn excess highlights a disturbance of anthocyanin accumulation, and tolerance to *B. cinerea* reveals cuticle permeability

Visual inspection of mature plants showed that WT plants accumulated anthocyanins upon Zn treatment whereas rosette leaves of amiRNA plants did not seem to do so, whatever the growth condition (Fig. 5A). Parallel kinetic quantification of shoot anthocyanins showed that anthocyanins were similarly detected in WT and amiRNA plants grown under the control condition (Fig. 5B). However, two to three days after the start of Zn exposure, anthocyanins started to accumulate in WT plants but no change was observed in amiRNA plants (Fig. 5B). On the other hand, the unexpected tolerance of amiRNA lines to *B. cinerea* was reminiscent of observations on cuticle permeable mutants, e.g., *lacs2.3* and *bdg* (Bessire *et al.*, 2007; Tang *et al.*, 2007), *pec1* (Bessire *et al.*, 2011), *eca2* and *aba* (Blanc *et al.*, 2018). Consequently, we investigated cuticle permeability of the amiRNA lines. Toluidine blue tests indicated that the cuticle of the amiRNA lines was more permeable than the cuticle of the WT plants, and behaved like the *A. thaliana lacs2-3* cuticle mutant used as a control (Fig. 6A). Conversely, anthocyanins accumulated in the *Atlacs2-3* mutant under Zn excess conditions (Supplementary Fig. S13), but aboveground dry mass decreased in the same range as in the WT, and significantly differed from the increase dry mass characteristic of amiRNA plants (Fig. 6B).

Discussion

Plant defensins have been mostly studied for their antifungal activities, but they also perform additional roles *in vivo,* hence they display promiscuous features (Aharoni *et al.*, 2005; Nobeli *et al.*, 2009; Franco, 2011). However, studies exploring if decreased endogenous defensin expression can affect different activities are rare. We therefore, addressed here the effect of a decrease of endogenous *AtPDF1* transcripts (and corresponding proteins) engineered by amiRNA technology and tested its effect on the response of *A. thaliana* to different pathogens and different metal excess. Unexpectedly, the amiRNA plants exhibiting decreased expression of five *AtPDF1* transcripts were

unexpectedly found more tolerant to different pathogens (Fig. 2, Fig. 3) and their dry mass specifically increased in response to Zn excess exposure (Fig. 4A-B, Supplementary Fig. S10).

Variation of gene expression within the *AtPDF1* family

Within *AtPDF1* members, variation in expression has been documented according to the tissue, the developmental stage and/or cultivation conditions or in response to stress [(De Coninck *et al.*, 2010; Nguyen *et al.*, 2014); Supplementary Fig. S2B-C, Supplementary Table S4-S5 and S6)]. The present work also reports discrepancies in transcript and protein detection for some *AtPDF1*s: **i)** in both WT and amiRNA seedlings grown *in vitro*, *AtPDF1.2b* and *1.2c* transcripts were not detected (Fig. 1B, Supplementary Fig. S5), **ii)** *AtPDF1.5* transcripts was detected in seedlings grown *in vitro* (Fig. 1B, Supplementary Fig. S4) but not in mature plants grown in soil (Fig. 2C, Supplementary Fig. S9) and **iii)** no AtPDF1.4 and 1.5 specific peptide could be detected by MS/MS on any of the samples analyzed (seeds, seedlings and mature plants) and peptide identifying AtPDF1.2a and/or 1.2b and/or 1.2c and/or 1.3 detection could not be detected in mature plants (in coherence with information in public databases, see Supplementary Table S5 and S6). The origin of these discrepancies would need further investigations. Yet, they did not bias the fact that, in amiRNA lines, transcripts and proteins levels are decreased for the five most similar *AtPDF1* members *AtPDF1.1*, *1.2a*, *1.2b*, *1.2c* and *1.3* as compared to WT (Fig.1A-D) so that the phenotypic differences between the WT and the homozygous amiRNA lines generated for this study could be validated statistically and associated with endogenous *AtPDF1* expression decrease.

Functional specificity questioned among members of the *AtPDF1* family

The extensive phenotypic analysis of amiRNA plants presented here is novel. It highlights that decreased expression of the five most similar *AtPDF1*s is specifically associated with increased tolerance to different pathogens (Fig. 2, Fig. 3 and Supplementary Fig. S8 and S9) and with increased plant dry mass upon Zn (Fig. 4A-B and Supplementary Fig. S10 and S11). Still, it is difficult at present to predict if one or more amiRNA-targeted *PDF1* genes are more particularly involved in the response to one and/or the other stress, nor we can ascertain that expression of other *PDF*s and/or *DEFL*s is modified. A genome-wide transcript analysis of the 317 PDF and DEFLs inventoried genes (Silverstein *et al.*, 2005) would start to provide some indications. This should be completed by MS/MS analysis spanning the entire range of protein molecular weight (since we presented here the analysis of a 10 kDa fraction). In addition, this study shows that the seven *AtPDF1*s are not all equally involved in the plant response to pathogens and to Zn excess**. Expression of *AtPDF1.4* and *1.5* indeed increases Zn tolerance in yeast (Shahzad *et al.*, 2013), but no phenotype of the plant response to Zn excess or to pathogens was observed in the double null *Atpdf1.4-Atpdf1.5* mutant (Supplementary Fig. S10B and -D and Supplementary Fig. S8, respectively). The transcript levels of *AtPDF1.4* and *AtPDF1.5* were amongst the highest within the *AtPDF1* family members (Fig. 1B, Supplementary Fig. S5; Fig. 2C, Supplementary Fig. S9), but they did not compensate for the dominant amiRNA plant growth phenotypes in Zn excess conditions (Fig. 4A-B) and the increased tolerance to pathogens (Fig. 2A-B and Fig. 3). At present, we cannot totally rule out that these *AtPDF1.4* and *1.5* genes could have undergone a neo-functional evolutionary fate, so that they can be endowed with a new function

other than the response to pathogens and/or Zn excess. This hypothesis is supported by the suggested role of *AtPDF1.5* in nitrogen nutrition and Cd stress (Wu *et al.*, 2021).

Decrease in endogenous *AtPDF1* expression: a by-pass to confer tolerance to pathogens?

We show here that amiRNA plants are affected in cuticle permeability (Fig. 6A). Changes in cuticle permeability such as those observed in the *lacs2*, *bdg* and *eca2* mutants (Kurdyukov *et al.*, 2006) have been associated with resistance to *B. cinerea* and other major pathogens including *P. synringae* pv *maculicola* (Bessire *et al.*, 2007; Chassot *et al.*, 2007; Blanc *et al.*, 2018). This has been linked to higher ROS production in cuticle mutants (L'Haridon *et al.*, 2011), but also to distinct phyllosphere microbiome populations in WT plants and cuticle mutants (Ritpitakphong *et al.*, 2016). In this regards, knowing whether amiRNA transgenics accumulate more ROS and/or if their phyllosphere microbiome populations differs from WT would be of interest (Bi *et al.*, 2023). Increased tolerance of amiRNA plants to *H. arabidopsdis* seems unlikely related to cuticle permeability because the *lacs2.3* mutant was as susceptible as the WT plants to this pathogen (Supplementary Fig. S8). Still, this hypothesis cannot be totally ruled out since different cuticle mutants can behave differently in response to a single pathogen (Ziv *et al.*, 2018; Aragon *et al.*, 2021). Increased plant tolerance to pathogens has been described in various situations affecting hormonal signalling (Sanchez-Vallet *et al.*, 2012; Liu *et al.*, 2016), metabolic reprogramming or structural modifications (Eschen-Lippold *et al.*, 2012; Taurino *et al.*, 2014; AbuQamar *et al.*, 2017; Sham *et al.*, 2017). However, it has been suggested that resistance of cuticle mutants can also be attributed to the induction of additional defence pathways, beyond the canonical ones (Aragon *et al.*, 2021). Concomitant tolerance to different pathogens is thus complex and multi-layered. Therefore, it would be highly interesting to conduct a comparative investigation between the wild-type (WT) and amiRNA genotypes using a multi-OMIC approach including transcript and metabolomic analysis. This could shed light on the putative links between *PDF1* decrease cuticle permeability and tolerance to different pathogens.

A role of *AtPDF1*s in the interplay between plant growth and response to Zn excess?

When plants are exposed to high Zn levels in their environment, they face the need to maintain Zn homeostasis. This is achieved through a regulated crosstalk between processes of transmembrane transport, cellular uptake, export and subcellular compartmentalisation, and chelation of free ions by small organic molecules, peptides and proteins (Clemens, 2001; Verbruggen *et al.*, 2009; Lin & Aarts, 2012; Sinclair & Kramer, 2012). In response to Zn excess, ectopic expression of *PDF1* in *A. thaliana* seedlings, cultivated *in vitro* axenic conditions, resulted in better tolerance, but this process cannot be related to the above-mentioned homeostasis mechanisms (Mirouze *et al.*, 2006; Mith *et al.*, 2015). When cultivated in similar *in vitro* axenic conditions, amiRNA seedlings were more sensitive than the WT and double null *Atpdf1.4-Atpdf1.5* mutant to Zn excess (Supplementary Fig. S10A-B). Therefore, a correlation exists between *PDF1* expression and Zn tolerance in seedlings germinated in the presence of Zn in axenic conditions. This brings some mechanistic coherence to a process that still remains to be causally elucidated. Interestingly, during plant growth, ectopic expression of *PDF1* did not provide zinc tolerance to transgenic over-expressing plants (OE *AhPDF1.1b*), which behaved like the WT and the double null *Atpdf1.4-Atpdf1.5* mutant (Supplementary Fig. S10C-D). A similar behaviour has been reported for the *SNAKIN* AMP (*SN1*),

where *SN1* over-expressing lines were phenotypically indistinguishable from the WT control (Nahirnak *et al.*, 2012), whereas silenced lines were affected in their growth and development (Almasia *et al.*, 2020). In this context, we report here a new property of *PDF1* with respect to Zn tolerance where decreased expression of endogenous *AtPDF1* transcripts interferes directly or indirectly with the plant balance between growth and the Zn excess response, resulting in continuous shoot growth during stress.

As a general process, the trade-off between growth and stress resistance involves specialised molecular mechanisms that target reduced resource consumption resulting in increased fitness (Campos *et al.*, 2016; Major *et al.*, 2017; Bechtold & Field, 2018; Chen *et al.*, 2021; Ogawa-Ohnishi *et al.*, 2022). There are indications that this process results from the suppression of growth by stress signalling pathways as an adaptive strategy to maximize survival (Zhang *et al.*, 2020). Under Zn excess conditions, we noted a time point when mature WT plant growth was reduced, whereas amiRNA plant growth was not affected. Most surprisingly, amiRNA plants maintained growth and leaf production under Zn excess (Fig. 4A-B). This unbalanced response between growth and the response to Zn excess was specific to the five AtPDF1-amiRNA silencing (Supplementary Fig. S10D) and was specific to Zn excess as compared to the other metals tested (Supplementary Fig. S11). Moreover, no difference in Zn content was noted between the WT and amiRNA plants (Fig. 4C). Based on studies mostly performed on metal-hyperaccumulating species, we know that Zn is not evenly distributed among tissues, nor it is found as a single molecular species (Küpper *et al.*, 1999; Sarret *et al.*, 2009; Haydon, 2014; Kozhevnikova *et al.*, 2017). Since we cannot rule out that these modifications could impact Zn toxicity, it would thus be interesting to further investigate and compare these Zn characteristics in WT and amiRNA plants.

Disturbance in stress signalling and development in amiRNA plants

Several characteristics observed in amiRNA plants suggest that stress signalling and development might be disrupted at several levels. First, anthocyanins are known to accumulate in plants exposed to abiotic stress (Dixon & Paiva, 1995; Kovinich *et al.*, 2015). Among their numerous roles (Gould, 2004), they act on cellular protection from oxidative damage (Chalker-Scott, 1999; Agati *et al.*, 2012) and protect the photosynthetic apparatus (Xu *et al.*, 2017; Xu & Rothstein, 2018). This occurs in particular upon metal exposure, as evidenced in the extremophiles *A. halleri* and *A. arenosa*, in which exposure to high Cd or Zn decreases the chlorophyll content and increases the anthocyanin content in leaves compared to the control (Szopinski *et al.*, 2019). This has also been nicely shown in Cd excluder *A. halleri* populations, where flavonoid accumulation appears important to cope with Cd toxicity as compared to Cd hyperaccumulator populations (Corso *et al.*, 2018). WT *A. thaliana* plants accumulated anthocyanins shortly after Zn exposure, but amiRNA plants did not (Fig. 5). In this respect, the pale green colour of the amiRNA lines upon aging (Supplementary Fig. S7C) might be indicative of damage to the photosynthetic apparatus due to poor anthocyanin accumulation. Second, specific leaf area [(*i.e.*, the light-capturing surface area *per* unit of dry mass that is a proxy of fundamental plant functions such as net photosynthetic capacity, growth rate and development rate (Vasseur *et al.*, 2012; Sartori *et al.*, 2019)] was significantly higher in amiRNA plants (Supplementary Fig. S7D), indicating faster development and/or an earlier flowering phenotype than the WT (Sartori *et al.*, 2019). In this regard, early flowering can also be considered as a stress-induced response, a third category of flowering response in addition to photoperiodic flowering and vernalisation (Riboni

et al., 2014; Kazan & Lyons, 2016; Park *et al.*, 2016). And indeed, amiRNA plants flower before WT plants (Supplementary Fig. S7A-B). Third, amiRNA plants had a more permeable cuticle than WT plants, suggesting that decrease of various defensin expression – could ultimately alter cell wall and/or plasma membranes constituents with consequences on development and stress sensing (Rui & Dinneny, 2020). Fourth, amiRNA plants were more tolerant to pathogens with different life styles, i.e., a necrotrophic fungus, a hemibiotrophic bacterium and an obligate biotrophic oomycete (Fig. 2 and Fig. 3), although resistance to these pathogens is thought to be mediated by different signalling pathways (Zhang *et al.*, 2018; Li *et al.*, 2019). A more general mechanism probably occurs in these plants, possibly related to a global disruption of stress signalling.

Overall, the convergence of these observations, could point to some basic intrinsic stress signalling disruption in amiRNA plants leading to increased tolerance to biotic and abiotic stresses. Finally, if Zn excess is not perceived correctly by amiRNA plants, this could alter the fine tuning of the stress response and growth of plants, and tip the scales towards growth. Interestingly, studies on *SNAKIN SN1* have shown that it potentially integrates development and defence signals directly and/or indirectly by modulating protein activity, modifying the hormonal balance and/or participating in redox regulation (Nahirnak *et al.*, 2012; Almasia *et al.*, 2020). Thus, it still remains to be clarified whether and how *PDF1*-expression-dependent defence mechanisms are finely tuned to overcome a given stress. More specifically, regarding the behaviour of amiRNA plants presented in this work, the way the observed stress perception disruptions are translated at the molecular level will remain to be investigated, and the unexpected phenotypes will have to be re-evaluated with CRISPR-edited plants where expression of the five most similar *AtPDF1*s will be totally inactivated.

Functional promiscuity of a single protein: one or several pathway(s)?

Plant defensins and DEFLs by extension are recognised as promiscuous proteins, but studies explaining how one protein can display such functional diversity are still rare. Recent analyses have shown that *Medicago truncatula* defensin MtDef4 inhibits the growth of two ascomycete fungi – *Neurospora crassa* and *Fusarium graminearum* – *via* different mechanisms (El-Mounadi *et al.*, 2016). In addition, differences have been highlighted in the fungal and tumour cell killing mechanisms of a *Nicociana alata* defensin (Bleackley *et al.*, 2016). This exemplifies that the promiscuous nature of defensins can be evidenced through different mechanisms for one or several activities. Cuticle permeability was affected in amiRNA lines (Fig. 6A); this could at least explain their tolerance to *B. cinerea*. Conversely, the relative dry masses of the WT and the cuticle permeability *lacs2-3* mutant were similarly affected upon Zn excess (Fig. 6B), and differed from the continuous growth of amiRNA lines. Overall, in amiRNA plant, tolerance to *B. cinerea* may well be disconnected from the disrupted balance between growth and the plant response to Zn excess. The *lacs2*-3 mutant also accumulated anthocyanins (Supplementary Fig. S13), a characteristic of WT plants under Zn excess not found in amiRNA lines. In this regard, it might be interesting to observe the Zn excess behaviour of *A. thaliana* anthocyanin biosynthetic and/or signalling mutants (Xu *et al.*, 2015) to investigate if there is any causal relationship between these two processes.

Conclusion-Perspectives

Molecular and phenotypic characterisation of amiRNA lines highlight that a specific decrease in five out of seven *AtPDF1* increases tolerance to abiotic (Zn) and biotic (pathogen) stresses. These findings are unexpected and further studies are necessary to clarify their underlying mechanisms. CRISPR-edited plant analysis, as well as genome-wide investigations using multi-OMIC approaches (including transcriptomic, proteomic, and metabolomic analyses) would be of great interest in understanding why a lack of *AtPDF1* expression potentially affects stress perception and signalling integration under conditions of Zn excess and pathogen attack. It would also be most interesting to investigate whether *PDF1* silencing in Zn-hyperaccumulating plants results in better foliar growth since the production of aboveground biomass by these species has always been a limiting factor for the application of these traits, e.g., in soil phytoremediation.

Acknowledgements

Author's contributions

T.N.N.Nguyen designed the amiRNA constructs targeting the specific decrease of the accumulation of 5 *AtPDF1* transcripts, engineered *A. thaliana* amiRNA lines and characterised them at the molecular level; isolated and characterised the single *Atpdf1.4* and *Atpdf1.5* mutants and constructed the double *Atpdf1.4- Atpdf1.5* mutant, performed the comparative qRT-PCR analysis of *AtPDF1* transcripts on seedlings of wild-type, amiRNA and double *Atpdf1.4- Atpdf1.5* mutant plants. **O.Lamotte** designed and analysed the plant pathogenesis assays, performed *B. cinerea* pathogenesis and cuticle permeability tests and wrote the manuscript. **M.Alsulaiman** performed automated and manual phenotypic analysis of *AtPDF1* amiRNA plants in response to zinc and other metals in hydroponic and soil cultivation systems, and performed the analysis of plant traits (Zn, Fe and Mn content, anthocyanin dosage and SLA measurements)**. S.Ruffel** and **G.Krouk** provided their expertise in gene expression regulation. **N.Berger** performed the Mass Spectrometry comparative proteomic experiments and analysis. **V.Demolombe-Liozu** analyse proteomic data and performed statistical analysis. **C.Nespoulous** provide expertise on defensin protein detection. **T.M.N.Dang** performed the comparative qRT-PCR analysis of *AtPDF1* transcripts on wild-type and amiRNA plants in response to *B. cinerea* infection. **S.Aimé** performed *H. peronospora* and *P. synringae* pv *maculicola* pathogenesis tests. **P.Berthomieu** provided expertise on defensins and zinc tolerance. **C. Dubos** provided expertise on the plant metal response. **D.Wendehenne** provided expertise on the plant response to pathogens. **D.Vile** designed, supervised and analysed the *AtPDF1* amiRNA line phenotyping experiment, performed the statistical analysis of the results, drew the related figures and wrote the manuscript. **F.Gosti** designed, supervised and analysed the *AtPDF1* amiRNA lines construction and phenotyping experiment, performed the comparative flowering phenotyping study, consolidated qRT-PCR analysis and phenotyping experiment on OE *PDF1* transgenics, wrote the manuscript and consolidated each contributor's writing. **D.Vile** and **F.Gosti** agree to serve as co-last authors. **F.Gosti** agrees to serve as contact author and ensure communication.

Conflict of Interest

No conflict of interest declared.

Funding statement

Data Availability Statement

All experimental settings, data acquisitions and biological replicates are described in Supplementary Dataset S1 and all raw data are present in the Supplementary Dataset S2 file and are openly available online (https://doi.org/10.15454/AXY7FV) and proteomic data are available via ProteomeXchange with identifier PXD037695.

References

AbuQamar S, Moustafa K, Tran LS. **2017**. Mechanisms and strategies of plant defense against *Botrytis cinerea*. *Critical Reviews in Biotechnology* **37**(2): 262-274.

Aerts AM, Francois IE, Meert EM, Li QT, Cammue BP, Thevissen K. **2007**. The antifungal activity of RsAFP2, a plant defensin from *raphanus sativus*, involves the induction of reactive oxygen species in *Candida albicans*. *Microbial Physiology* **13**(4): 243-247.

Agati G, Azzarello E, Pollastri S, Tattini M. **2012**. Flavonoids as antioxidants in plants: location and functional significance. *Plant Science* **196**: 67-76.

Aharoni A, Gaidukov L, Khersonsky O, Mc QGS, Roodveldt C, Tawfik DS. **2005**. The 'evolvability' of promiscuous protein functions. *Nature Genetetics* **37**(1): 73-76.

Ahuja I, de Vos RC, Bones AM, Hall RD. **2010**. Plant molecular stress responses face climate change. *Trends in Plant Science* **15**(12): 664-674.

Almasia NI, Nahirnak V, Hopp HE, Vazquez-Rovere C. 2020. Potato Snakin-1: an antimicrobial player of the trade-off between host defense and development. *Plant Cell Reports* **39**(7): 839-849.

Andersen CL, Jensen JL, Ørntoft TF. **2004**. Normalization of Real-Time Quantitative Reverse Transcription-PCR Data: A Model-Based Variance Estimation Approach to Identify Genes Suited for Normalization, Applied to Bladder and Colon Cancer Data Sets. *Cancer Research* **64**(15): 5245.

Aragon W, Formey D, Aviles-Baltazar NY, Torres M, Serrano M. 2021. *Arabidopsis thaliana* Cuticle Composition Contributes to Differential Defense Response to *Botrytis cinerea*. *Frontiers in Plant Science* **12**: 738949.

Baxter AA, Richter V, Lay FT, Poon IK, Adda CG, Veneer PK, Phan TK, Bleackley MR, Anderson MA, Kvansakul M, et al. 2015. The tomato Defensin TPP3 binds Phosphatidylinositol (4,5)-Bisphosphate *via* a conserved dimeric cationic grip conformation to mediate cell lysis. *Molecular and Cellular Biololgy* **35**(11): 1964-1978.

Becher M, Talke IN, Krall L, Kramer U. **2004**. Cross-species microarray transcript profiling reveals high constitutive expression of metal homeostasis genes in shoots of the zinc hyperaccumulator *Arabidopsis halleri*. *The Plant Journal* **37**(2): 251-268.

Bechtold U, Field B. **2018**. Molecular mechanisms controlling plant growth during abiotic stress. *Journal of Experimental Botany* **69**(11): 2753-2758.

Berens ML, Wolinska KW, Spaepen S, Ziegler J, Nobori T, Nair A, Kruler V, Winkelmuller TM, Wang Y, Mine A, et al. 2019. Balancing trade-offs between biotic and abiotic stress responses

through leaf age-dependent variation in stress hormone cross-talk. *Proceedings of the National Academy of Sciences U S A* **116**(6): 2364-2373.

Berger N, Vignols F, Przybyla-Toscano J, Roland M, Rofidal V, Touraine B, Zienkiewicz K, Couturier J, Feussner I, Santoni V, *et al.* **2020**. Identification of client iron-sulfur proteins of the chloroplastic NFU2 transfer protein in *Arabidopsis thaliana*. *Journal of Experimental Botany* **71**(14): 4171-4187.

Berger N, Demolombe V, Hem S, Rofidal V, Steinmann L, Krouk G, Crabos A, Nacry P, Verdoucq L, Santoni V. **2022**. Root Membrane Ubiquitinome under Short-Term Osmotic Stress. *International Journal of Molecular Sciences* **23**(4).

Bessire M, Borel S, Fabre G, Carraca L, Efremova N, Yephremov A, Cao Y, Jetter R, Jacquat AC, Metraux JP, et al. **2011**. A member of the PLEIOTROPIC DRUG RESISTANCE family of ATP binding cassette transporters is required for the formation of a functional cuticle in Arabidopsis. *The Plant Cell* **23**(5): 1958-1970.

Bessire M, Chassot C, Jacquat AC, Humphry M, Borel S, Petétot JMC, Métraux JP, Nawrath C. **2007**. A permeable cuticle in *Arabidopsis* leads to a strong resistance to *Botrytis cinerea*. *The EMBO Journal* **26**(8): 2158-2168.

Bi K, Liang Y, Mengiste T, Sharon A. **2023**. Killing softly: a roadmap of *Botrytis cinerea* pathogenicity. *Trends in Plant Science* **28**(2): 211-222.

Blanc C, Coluccia F, L'Haridon F, Torres M, Ortiz-Berrocal M, Stahl E, Reymond P, Schreiber L, Nawrath C, Metraux JP, et al. **2018**. The cuticle mutant *eca2* modifies plant defense responses to biotrophic and necrotrophic pathogens and herbivory insects. *Molecular Plant-Microbe Interactions* **31**(3): 344-355.

Bleackley MR, Payne JA, Hayes BM, Durek T, Craik DJ, Shafee TM, Poon IK, Hulett MD, van der Weerden NL, Anderson MA. **2016**. *Nicotiana alata* defensin chimeras reveal differences in the mechanism of fungal and tumor cell killing and an enhanced antifungal variant. *Antimicrobial Agents and Chemotherapy* **60**(10): 6302-6312.

Bradford MM. **1976**. A rapid and sensitive method for the quantitation of microgram quantities of protein utilizing the principle of protein-dye binding. *Analytical Biochemistry* **72**: 248-254.

Campos ML, Yoshida Y, Major IT, de Oliveira Ferreira D, Weraduwage SM, Froehlich JE, Johnson BF, Kramer DM, Jander G, Sharkey TD, et al. **2016**. Rewiring of jasmonate and phytochrome B signalling uncouples plant growth-defense tradeoffs. *Nature Communications* **7**: 12570.

Carvalho AdO, Gomes VM. **2009**. Plant defensins-prospects for the biological functions and biotechnological properties. *Peptides* **30**: 1007-1020.

Carvalho AdO, Gomes VM. **2011**. Plant Defensins and Defensin-Like Peptides - Biological Activities and Biotechnological Applications. *Current Pharmaceutical Design* **17**: 4270-4293.

Chalker-Scott L. **1999**. Environmental Significance of Anthocyanins in Plant Stress Responses. *Photochemistry and Photobiology* **70**(1): 1-9.

Chassot C, Nawrath C, Metraux JP. **2007**. Cuticular defects lead to full immunity to a major plant pathogen. *The Plant Journal* **49**(6): 972-980.

Chen H, Bullock DA, Jr., Alonso JM, Stepanova AN. **2021**. To Fight or to Grow: The Balancing Role of Ethylene in Plant Abiotic Stress Responses. *Plants (Basel, Switzerland)* **11**(1): 33.

Clemens S. **2001**. Molecular mechanisms of plant metal tolerance and homeostasis. *Planta* **212**(4): 475-486.

Clough SJ, Bent AF. **1998**. Floral dip: a simplified method for Agrobacterium-mediated transformation of *Arabidopsis thaliana*. *The Plant Journal* **16**(6): 735-743.

Corso M, Schvartzman MS, Guzzo F, Souard F, Malkowski E, Hanikenne M, Verbruggen N. **2018**. Contrasting cadmium resistance strategies in two metallicolous populations of *Arabidopsis halleri*. *New Phytologist* **218**(1): 283-297.

Cox J, Mann M. **2008**. MaxQuant enables high peptide identification rates, individualized p.p.b.-range mass accuracies and proteome-wide protein quantification. *Nature Biotechnoly* **26**(12): 1367-1372.

Cox J, Neuhauser N, Michalski A, Scheltema RA, Olsen JV, Mann M. **2011**. Andromeda: A Peptide Search Engine Integrated into the MaxQuant Environment. *Journal of Proteome Research* **10**(4): 1794-1805.

Czechowski T, Stitt M, Altmann T, Udvardi MK, Scheible WR. **2005**. Genome-wide identification and testing of superior reference genes for transcript normalization in Arabidopsis. *Plant Physiology* **139**(1): 5-17.

De Coninck B, Cammue BPA, Thevissen K. **2013**. Modes of antifungal action and *in planta* functions of plant defensins and defensin-like peptides. *Fungal Biology Reviews* **26**(4): 109-120.

De Coninck BM, Sels J, Venmans E, Thys W, Goderis IJ, Carron D, Delaure SL, Cammue BP, De Bolle MF, Mathys J. **2010**. *Arabidopsis thaliana* plant defensin AtPDF1.1 is involved in the plant response to biotic stress. *New Phytologist* **187**(4): 1075-1088.

de Souza Candido E, Silva Cardoso MH, Sousa DA, Viana JC, de Oliveira-Junior NG, Miranda V, Franco OL. **2014**. The use of versatile plant antimicrobial peptides in agribusiness and human health. *Peptides* **55**: 65-78.

Denance N, Sanchez-Vallet A, Goffner D, Molina A. **2013**. Disease resistance or growth: the role of plant hormones in balancing immune responses and fitness costs. *Frontiers in Plant Science* **4**: 155.

Dixon RA, Paiva NL. **1995**. Stress-Induced Phenylpropanoid Metabolism. *The Plant Cell* **7**(7): 1085-1097.

Dos Santos IS, Carvalho Ade O, de Souza-Filho GA, do Nascimento VV, Machado OL, Gomes VM. **2010**. Purification of a defensin isolated from *Vigna unguiculata* seeds, its functional expression in *Escherichia coli,* and assessment of its insect alpha-amylase inhibitory activity. *Protein Expression and Purification* **71**(1): 8-15.

Edgar RC. **2004**. MUSCLE: Multiple sequence alignment with high accuracy and high throughput. *Nucleic Acids Research* **32**(5): 1792-1797.

El-Mounadi K, Islam KT, Hernandez-Ortiz P, Read ND, Shah DM. **2016**. Antifungal mechanisms of a plant defensin MtDef4 are not conserved between the ascomycete fungi *Neurospora crassa* and *Fusarium graminearum*. *Molecular Microbiology* **100**(3): 542-559.

Eschen-Lippold L, Landgraf R, Smolka U, Schulze S, Heilmann M, Heilmann I, Hause G, Rosahl S. **2012**. Activation of defense against *Phytophthora infestans* in potato by down-regulation of syntaxin gene expression. *New Phytologist* **193**(4): 985-996.

Foyer CH, Rasool B, Davey JW, Hancock RD. **2016**. Cross-tolerance to biotic and abiotic stresses in plants: a focus on resistance to aphid infestation. *Journal of Experimental Botany* **67**(7): 2025-2037.

Franco OL. **2011**. Peptide promiscuity: an evolutionary concept for plant defense. *Federation of European Biochemical Societies Letters* **585**(7): 995-1000.

Fujita M, Fujita Y, Noutoshi Y, Takahashi F, Narusaka Y, Yamaguchi-Shinozaki K, Shinozaki K. **2006**. Crosstalk between abiotic and biotic stress responses: a current view from the points of convergence in the stress signaling networks. *Current Opinion in Plant Biology* **9**(4): 436-442.

Gachomo EW, Jimenez-Lopez JC, Kayode AP, Baba-Moussa L, Kotchoni SO. **2012**. Structural characterization of plant defensin protein superfamily. *Molecular Biology Reports* **39**(4): 4461-4469.

Gao AG, Hakimi SM, Mittanck CA, Wu Y, Woerner BM, Stark DM, Shah DM, Liang J, Rommens CM. **2000**. Fungal pathogen protection in potato by expression of a plant defensin peptide. *Nature Biotechnology* **18**(12): 1307-1310.

Gaspar YM, McKenna JA, McGinness BS, Hinch J, Poon S, Connelly AA, Anderson MA, Heath RL. **2014**. Field resistance to *Fusarium oxysporum* and *Verticillium dahliae* in transgenic cotton expressing the plant defensin NaD1. *Journal of Experimental Botany* **65**(6): 1541-1550.

Gould KS. **2004**. Nature's Swiss Army Knife: The Diverse Protective Roles of Anthocyanins in Leaves. *Journal of Biomedicine and Biotechnology* **2004**(5): 314-320.

Gu T-Y, Qi Z-A, Chen S-Y, Yan J, Fang Z-J, Wang J-M, Gong J-M. **2022**. Dual-function DEFENSIN 8 mediates phloem cadmium unloading and accumulation in rice grains. *Plant Physiology*. https://doi.org/10.1093/plphys/kiac423

Hammond JP, Bowen HC, White PJ, Mills V, Pyke KA, Baker AJ, Whiting SN, May ST, Broadley MR. **2006**. A comparison of the *Thlaspi caerulescens* and *Thlaspi arvense* shoot transcriptomes. *New Phytologist* **170**(2): 239-260.

Haydon MJ. **2014**. Getting a sense for zinc in plants. *New Phytologist* **202**(1): 10-12.

Hellens RP, Edwards EA, Leyland NR, Bean S, Mullineaux PM. **2000**. pGreen: a versatile and flexible binary Ti vector for *Agrobacterium*-mediated plant transformation. *Plant Molecular Biology* **42**(6): 819-832.

Hiruma K, Takano Y. **2011**. Roles of *EDR1* in non-host resistance of Arabidopsis. *Plant Signaling & Behavior* **6**(11): 1831-1833.

Hsiao PY, Cheng CP, Koh KW, Chan MT. **2017**. The Arabidopsis defensin gene, *AtPDF1.1,* mediates defence against *Pectobacterium carotovorum* subsp. *carotovorum via* an iron-withholding defence system. *Scientific Reports* **7**(1): 9175.

Islam KT, Velivelli SLS, Berg RH, Oakley B, Shah DM. **2017**. A novel bi-domain plant defensin MtDef5 with potent broad-spectrum antifungal activity binds to multiple phospholipids and forms oligomers. *Sci Rep* **7**(1): 16157.

Katagiri F, Thilmony R, He SY. **2002**. The *Arabidopsis thaliana-Pseudomonas Syringae* Interaction. *The Arabidopsis Book* **2002**(1).

Kaur P, Jost R, Sivasithamparam K, Barbetti MJ. **2011b**. Proteome analysis of the *Albugo candida-Brassica juncea* pathosystem reveals that the timing of the expression of defence-related genes is a crucial determinant of pathogenesis. *Journal of Experimental Botany* **62**(3): 1285-1298.

Kaur J, Sagaram US, Shah D. **2011a**. Can plant defensins be used to engineer durable commercially useful resistance in crop plants? *Fungal Biology Reviews* **25**: 128-135.

Kaur J, Thokala M, Robert-Seilaniantz A, Zhao P, Peyret H, Berg H, Pandey S, Jones J, Shah D. **2012**. Subcellular targeting of an evolutionarily conserved plant defensin MtDef4.2 determines the outcome of plant-pathogen interaction in transgenic Arabidopsis. *Molecular Plant Pathology* **13**(9): 1032-1046.

Kazan K, Lyons R. **2016**. The link between flowering time and stress tolerance. *Journal of Experimental Botany* **67**(1): 47-60.

Klepikova AV, Kasianov AS, Gerasimov ES, Logacheva MD, Penin AA. **2016**. A high resolution map of the *Arabidopsis thaliana* developmental transcriptome based on RNA-seq profiling. *The Plant Journal* **88**(6): 1058-1070.

Koncz C, Schell J. **1986**. The promoter of T$_L$-DNA gene 5 controls the tissue-specific expression of chimaeric genes carried by a novel type of *Agrobacterium* binary vector. *Molecular and General Genetics* **204**: 383-396.

Kovinich N, Kayanja G, Chanoca A, Otegui MS, Grotewold E. **2015**. Abiotic stresses induce different localizations of anthocyanins in Arabidopsis. *Plant Signaling & Behavior* **10**(7): e1027850.

Kozhevnikova AD, Seregin IV, Gosti F, Schat H. **2017**. Zinc accumulation and distribution over tissues in *Noccaea caerulescens* in nature and in hydroponics: a comparison. *Plant and Soil* **411**: 5-16.

Küpper H, Jie Zhao F, McGrath SP. **1999**. Cellular Compartmentation of Zinc in Leaves of the Hyperaccumulator *Thlaspi caerulescens*. *Plant Physiology* **119**(1): 305.

Kurdyukov S, Faust A, Nawrath C, Bar S, Voisin D, Efremova N, Franke R, Schreiber L, Saedler H, Metraux JP, et al. 2006. The epidermis-specific extracellular BODYGUARD controls cuticle development and morphogenesis in Arabidopsis. *The Plant Cell* **18**(2): 321-339.

Kvansakul M, Lay FT, Adda CG, Veneer PK, Baxter AA, Phan TK, Poon IK, Hulett MD. **2016**. Binding of phosphatidic acid by NsD7 mediates the formation of helical defensin-lipid oligomeric assemblies and membrane permeabilization. *Proceedings of the National Academy of Sciences U S A* **113**(40): 11202-11207.

L'Haridon F, Besson-Bard A, Binda M, Serrano M, Abou-Mansour E, Balet F, Schoonbeek HJ, Hess S, Mir R, Leon J, et al. 2011. A permeable cuticle is associated with the release of reactive oxygen species and induction of innate immunity. *Public Library of Science Pathogens* **7**(7): e1002148.

La Camera S, L'Haridon F, Astier J, Zander M, Abou-Mansour E, Page G, Thurow C, Wendehenne D, Gatz C, Metraux JP, et al. 2011. The glutaredoxin ATGRXS13 is required to facilitate *Botrytis cinerea* infection of *Arabidopsis thaliana* plants. *The Plant Journal* **68**(3): 507-519.

Lacerda AF, Vasconcelos EA, Pelegrini PB, Grossi de Sa MF. **2014**. Antifungal defensins and their role in plant defense. *Frontiers in Microbiology* **5**: 116.

Lay FT, Anderson MA. **2005**. Defensins-components of the innate immune system in plants. *Current Protein and Peptide Science* **6**(1): 85-101.

Lehrer RI. **2004**. Primate defensins. *Nature Reviews Microbiology* **2**(9): 727-738.

Li N, Han X, Feng D, Yuan D, Huang L-J. 2019. Signaling Crosstalk between Salicylic Acid and Ethylene/Jasmonate in Plant Defense: Do We Understand What They Are Whispering? International Journal of Molecular Sciences **20**(3): 671.

Li Y, Han J, Wu J, Li D, Yang X, Huang A, Bu G, Meng F, Kong F, Cao X, et al. 2020. Transcriptome-based evaluation and validation of suitable housekeeping gene for quantification real-time PCR under specific experiment condition in teleost fishes. *Fish Shellfish Immunol* **98**: 218-223.

Lin YF, Aarts MG. **2012**. The molecular mechanism of zinc and cadmium stress response in plants. *Cellular and Molecular Life Sciences* **69**(19): 3187-3206.

Liu Y, Huang X, Li M, He P, Zhang Y. **2016**. Loss-of-function of *Arabidopsis* receptor-like kinase BIR1 activates cell death and defense responses mediated by BAK1 and SOBIR1. *New Phytologist* **212**(3): 637-645.

Liu YJ, Cheng CS, Lai SM, Hsu MP, Chen CS, Lyu PC. **2006**. Solution structure of the plant defensin VrD1 from mung bean and its possible role in insecticidal activity against bruchids. *Proteins* **63**(4): 777-786.

Luo J-S, Yang Y, Gu T, Wu Z, Zhang Z. **2019a**. The Arabidopsis defensin gene *AtPDF2.5* mediates cadmium tolerance and accumulation. *Plant, Cell and Environment* **42**(9): 2681-2695.

Luo JS, Gu T, Yang Y, Zhang Z. **2019b**. A non-secreted plant defensin AtPDF2.6 conferred cadmium tolerance *via* its chelation in Arabidopsis. *Plant Molecular Biology* **100**(4-5): 561-569.

Luo JS, Huang J, Zeng DL, Peng JS, Zhang GB, Ma HL, Guan Y, Yi HY, Fu YL, Han B, et al. 2018. A defensin-like protein drives cadmium efflux and allocation in rice. *Nature Communication* **9**(1): 645.

Luo JS, Xiao Y, Yao J, Wu Z, Yang Y, Ismail AM, Zhang Z. **2020**. Overexpression of a Defensin-Like Gene *CAL2* Enhances Cadmium Accumulation in Plants. *Frontiers in Plant Science* **11**: 217.

Major IT, Yoshida Y, Campos ML, Kapali G, Xin XF, Sugimoto K, de Oliveira Ferreira D, He SY, Howe GA. **2017**. Regulation of growth-defense balance by the JASMONATE ZIM-DOMAIN (JAZ)-MYC transcriptional module. *New Phytologist* **215**(4): 1533-1547.

Mallory AC, Ely L, Smith TH, Marathe R, Anandalakshmi R, Fagard M, Vaucheret H, Pruss G, Bowman L, Vance VB. **2001**. HC-Pro suppression of transgene silencing eliminates the small RNAs but not transgene methylation or the mobile signal. *The Plant Cell* **13**(3): 571-583.

Melo FR, Rigden DJ, Franco OL, Mello LV, Ary MB, Grossi de Sa MF, Bloch C, Jr. 2002. Inhibition of trypsin by cowpea thionin: characterization, molecular modeling, and docking. *Proteins* **48**(2): 311-319.

Mergner J, Frejno M, List M, Papacek M, Chen X, Chaudhary A, Samaras P, Richter S, Shikata H, Messerer M, *et al*. 2020. Mass-spectrometry-based draft of the Arabidopsis proteome. Nature **579**(7799): 409-414.

Mirouze M, Sels J, Richard O, Czernic P, Loubet S, Jacquier A, Francois IE, Cammue BP, Lebrun M, Berthomieu P, et al. 2006. A putative novel role for plant defensins: a defensin from the zinc hyper-accumulating plant, *Arabidopsis halleri*, confers zinc tolerance. *The Plant Journal* **47**(3): 329-342.

Mith O, Benhamdi A, Castillo T, Berge M, MacDiarmid CW, Steffen J, Eide DJ, Perrier V, Subileau M, Gosti F, et al. 2015. The antifungal plant defensin AhPDF1.1b is a beneficial factor involved in adaptive response to zinc overload when it is expressed in yeast cells. *Microbiology Open* **4**(3): 409-422.

Murashige T, Skoog F. **1962**. A revised medium for rapid growth and bioassays with tobacco tissue cultures. *Physiologia. Plantarum* **15**: 473-497.

Nahirnak V, Almasia NI, Fernandez PV, Hopp HE, Estevez JM, Carrari F, Vazquez-Rovere C. **2012**. Potato *snakin-1* gene silencing affects cell division, primary metabolism, and cell wall composition. *Plant Physiology* **158**(1): 252-263.

Nakata M, Ohme-Takagi M. **2014**. Quantification of Anthocyanin Content. *Bio-protocol* **4**(7): e1098.

Nejat N, Mantri N. **2017**. Plant Immune System: Crosstalk Between Responses to Biotic and Abiotic Stresses the Missing Link in Understanding Plant Defence. *Current Issues in Molecular Biology* **23**: 1-16.

Nguyen NNT, Ranwez V, Vile D, Soulie MC, Dellagi A, Expert D, Gosti F. **2014**. Evolutionary Tinkering of the Expression of *PDF1s* Suggests their Joint Effect on Zinc Tolerance and the Response To Pathogen Attack. *Frontiers in Plant Science, 11 March 2014 | doi: 10.3389/fpls.2014.00070*(Special Topic on "Metal hyperaccumulation and hypertolerance: a model for plant evolutionary genomics").

Nobeli I, Favia AD, Thornton JM. **2009**. Protein promiscuity and its implications for biotechnology. *Nature Biotechnology* **27**(2): 157-167.

Ogawa-Ohnishi M, Yamashita T, Kakita M, Nakayama T, Ohkubo Y, Hayashi Y, Yamashita Y, Nomura T, Noda S, Shinohara H, et al. 2022. Peptide ligand-mediated trade-off between plant growth and stress response. *Science* **378**(6616): 175-180.

Osakabe Y, Osakabe K, Shinozaki K, Tran LS. **2014**. Response of plants to water stress. *Frontiers in Plant Science* **5**: 86.

Ossowski S, Schwab R, Weigel D. **2008**. Gene silencing in plants using artificial microRNAs and other small RNAs. *The Plant Journal* **53**(4): 674-690.

Oyinloye BE, Adenowo AF, Kappo AP. **2015**. Reactive Oxygen Species, Apoptosis, Antimicrobial Peptides and Human Inflammatory Diseases. *Pharmaceuticals* **8**(2): 151-175.

Padovan L, Scocchi M, Tossi A. **2010**. Structural aspects of plant antimicrobial peptides. *Current Protein and Peptide Science* **11**(3): 210-219.

Accepted Manuscript

Pandey P, Ramegowda V, Senthil-Kumar M. **2015**. Shared and unique responses of plants to multiple individual stresses and stress combinations: physiological and molecular mechanisms. *Frontiers in Plant Science* **6**: 723.

Parisi K, Shafee TMA, Quimbar P, van der Weerden NL, Bleackley MR, Anderson MA. **2019**. The evolution, function and mechanisms of action for plant defensins. *Seminars in Cell & Developmental Biology* **88**: 107-118.

Park HJ, Kim WY, Pardo JM, Yun DJ. **2016**. Molecular Interactions Between Flowering Time and Abiotic Stress Pathways. *International Review of Cell and Molecular Biology* **327**: 371-412.

Payne JA, Bleackley MR, Lee TH, Shafee TM, Poon IK, Hulett MD, Aguilar MI, van der Weerden NL, Anderson MA. **2016**. The plant defensin NaD1 introduces membrane disorder through a specific interaction with the lipid, phosphatidylinositol 4,5 bisphosphate. *Biochimica et Biophysica Acta* **1858**(6): 1099-1109.

Pelegrini PB, Lay FT, Murad AM, Anderson MA, Franco OL. **2008**. Novel insights on the mechanism of action of alpha-amylase inhibitors from the plant defensin family. *Proteins* **73**(3): 719-729.

Pieterse CM, Van der Does D, Zamioudis C, Leon-Reyes A, Van Wees SC. **2012**. Hormonal modulation of plant immunity. *Annual Review of Cell and Developmental Biology* **28**: 489-521.

Poon IKH, Baxter AA, Lay FT, Mills GD, Adda CG, Payne JAE, Phan TK, Ryan GF, White JA, Veneer PK, et al. **2014**. Phosphoinositide-mediated oligomerization of a defensin induces cell lysis. *Elife* **2014**(3).

RCoreTeam. **2020**. R: A language and environment for statistical computing. Vienna, Austria: R Foundation for Statistical Computing.

Rejeb IB, Pastor V, Mauch-Mani B. **2014**. Plant Responses to Simultaneous Biotic and Abiotic Stress: Molecular Mechanisms. *Plants (Basel)* **3**(4): 458-475.

Remans T, Smeets K, Opdenakker K, Mathijsen D, Vangronsveld J, Cuypers A. **2008**. Normalisation of real-time RT-PCR gene expression measurements in *Arabidopsis thaliana* exposed to increased metal concentrations. *Planta* **227**(6): 1343-1349.

Riboni M, Robustelli Test A, Galbiati M, Tonelli C, Conti L. **2014**. Environmental stress and flowering time: the photoperiodic connection. *Plant Signaling & Behavior* **9**(7): e29036.

Ritpitakphong U, Falquet L, Vimoltust A, Berger A, Metraux JP, L'Haridon F. **2016**. The microbiome of the leaf surface of Arabidopsis protects against a fungal pathogen. *New Phytologist* **210**(3): 1033-1043.

Rui Y, Dinneny JR. **2020**. A wall with integrity: surveillance and maintenance of the plant cell wall under stress. *New Phytologist* **225**(4): 1428-1439.

Rymaszewski W, Vile D, Bediee A, Dauzat M, Luchaire N, Kamrowska D, Granier C, Hennig J. **2017**. Stress-Related Gene Expression Reflects Morphophysiological Responses to Water Deficit. *Plant Physiology* **174**(3): 1913-1930.

Sagaram US, El-Mounadi K, Buchko GW, Berg HR, Kaur J, Pandurangi RS, Smith TJ, Shah DM. **2013**. Structural and functional studies of a phosphatidic acid-binding antifungal plant defensin MtDef4: identification of an RGFRRR motif governing fungal cell entry. *Public Library of Science One* **8**(12): e82485.

Sagaram US, Kaur J, Shah DM 2012. Antifungal plant defensins: structure -activity relationships, mode of action, and biotech applications. In: Rajasekaran K ed. Small wonders: peptides for disease control. Washinton, DC, USA: American Chemical Society, 317-336.

Sanchez-Vallet A, Lopez G, Ramos B, Delgado-Cerezo M, Riviere MP, Llorente F, Fernandez PV, Miedes E, Estevez JM, Grant M, et al. 2012. Disruption of abscisic acid signaling constitutively activates Arabidopsis resistance to the necrotrophic fungus *Plectosphaerella cucumerina*. *Plant Physiology* **160**(4): 2109-2124.

Sarret G, Willems G, Isaure MP, Marcus MA, Fakra SC, Frerot H, Pairis S, Geoffroy N, Manceau A, Saumitou-Laprade P. **2009**. Zinc distribution and speciation in *Arabidopsis halleri* x *Arabidopsis lyrata* progenies presenting various zinc accumulation capacities. *New Phytologist* **184**(3): 581-595.

Sartori K, Vasseur F, Violle C, Baron E, Gerard M, Rowe N, Ayala-Garay O, Christophe A, Jalon LG, Masclef D, et al. 2019. Leaf economics and slow-fast adaptation across the geographic range of *Arabidopsis thaliana*. *Scientific Report* **9**(1): 10758.

Schardl CL, Byrd AD, Benzion G, Altschuler MA, Hildebrand DF, Hunt AG. **1987**. Design and construction of a versatile system for the expression of foreign genes in plants. *Gene* **61**(1): 1-11.

Schneider CA, Rasband WS, Eliceiri KW. **2012**. NIH Image to ImageJ: 25 years of image analysis. *Nature Methods* **9**(7): 671-675.

Schwab R, Ossowski S, Riester M, Warthmann N, Weigel D. **2006**. Highly specific gene silencing by artificial microRNAs in Arabidopsis. *The Plant Cell* **18**(5): 1121-1133.

Schwab R, Palatnik JF, Riester M, Schommer C, Schmid M, Weigel D. **2005**. Specific effects of microRNAs on the plant transcriptome. *Developmental Cell* **8**(4): 517-527.

Sels J, Delaure SL, Aerts AM, Proost P, Cammue BP, De Bolle MF. **2007**. Use of a PTGS-MAR expression system for efficient *in planta* production of bioactive *Arabidopsis thaliana* plant defensins. *Transgenic Research* **16**(4): 531-538.

Sels J, Mathys J, De Coninck BM, Cammue BP, De Bolle MF. **2008**. Plant pathogenesis-related (PR) proteins: a focus on PR peptides. *Plant Physiology and Biochemistry* **46**(11): 941-950.

Shafee TM, Lay FT, Hulett MD, Anderson MA. **2016a**. The Defensins Consist of Two Independent, Convergent Protein Superfamilies. *Molecular Biology and Evolution* **33**(9): 2345-2356.

Shafee TM, Lay FT, Phan TK, Anderson MA, Hulett MD. **2017**. Convergent evolution of defensin sequence, structure and function. *Cellular and Molecular Life Sciences* **74**(4): 663-682.

Shafee TM, Robinson AJ, van der Weerden N, Anderson MA. **2016b**. Structural homology guided alignment of cysteine rich proteins. *Springerplus* **5**: 27.

Shahzad Z, Gosti F, Frerot H, Lacombe E, Roosens N, Saumitou-Laprade P, Berthomieu P. **2010**. The five *AhMTP1* zinc transporters undergo different evolutionary fates towards adaptive evolution to zinc tolerance in *Arabidopsis halleri*. *Public Library of Science Genetics* **6**(4): e1000911.

Shahzad Z, Ranwez V, Fizames C, Marques L, Le Martret B, Alassimone J, Gode C, Lacombe E, Castillo T, Saumitou-Laprade P, *et al.* 2013. *Plant Defensin type 1* (*PDF1*): protein promiscuity

and expression variation within the *Arabidopsis* genus shed light on zinc tolerance acquisition in *Arabidopsis halleri*. *New Phytologist* **200**(3): 820-833.

Sham A, Moustafa K, Al-Shamisi S, Alyan S, Iratni R, AbuQamar S. **2017**. Microarray analysis of Arabidopsis *WRKY33* mutants in response to the necrotrophic fungus *Botrytis cinerea*. *Public Library of Science One* **12**(2): e0172343.

Sher Khan R, Iqbal A, Malak R, Shehryar K, Attia S, Ahmed T, Ali Khan M, Arif M, Mii M. **2019**. Plant defensins: types, mechanism of action and prospects of genetic engineering for enhanced disease resistance in plants. *3 Biotech* **9**(5): 192.

Silverstein KA, Graham MA, Paape TD, VandenBosch KA. **2005**. Genome organization of more than 300 defensin-like genes in Arabidopsis. *Plant Physiology* **138**(2): 600-610.

Silverstein KA, Moskal WA, Jr., Wu HC, Underwood BA, Graham MA, Town CD, VandenBosch KA. **2007**. Small cysteine-rich peptides resembling antimicrobial peptides have been under-predicted in plants. *The Plant Journal* **51**(2): 262-280.

Sinclair SA, Kramer U. **2012**. The zinc homeostasis network of land plants. *Biochimica et Biophysica Acta* **1823**(9): 1553-1567.

Skirycz A, Inze D. **2010**. More from less: plant growth under limited water. *Current Opinion in Biotechnology* **21**(2): 197-203.

Slusarenko AJ, Schlaich NL. **2003**. Downy mildew of *Arabidopsis thaliana* caused by *Hyaloperonospora parasitica* (formerly *Peronospora parasitica*). *Molecular Plant Pathology* **4**(3): 159-170.

Stotz HU, Spence B, Wang Y. **2009**. A defensin from tomato with dual function in defense and development. *Plant Molecular Biology* **71**(1-2): 131-143.

Stotz HU, Waller F, Wang K 2013. Innate Immunity in Plants: The Role of Antimicrobial Peptides. In: Hiemstra PS, Zaat SAJ eds. Antimicrobial peptides and innate immunity. Basel, Switzerland: Springer Basel, 29-51.

Szopinski M, Sitko K, Gieron Z, Rusinowski S, Corso M, Hermans C, Verbruggen N, Malkowski E. **2019**. Toxic Effects of Cd and Zn on the Photosynthetic Apparatus of the *Arabidopsis halleri* and *Arabidopsis arenosa* Pseudo-Metallophytes. *Frontiers in Plant Science* **10**: 748.

Talke IN, Hanikenne M, Kramer U. **2006**. Zinc-dependent global transcriptional control, transcriptional deregulation, and higher gene copy number for genes in metal homeostasis of the hyperaccumulator *Arabidopsis halleri*. *Plant Physiology* **142**(1): 148-167.

Tang D, Simonich MT, Innes RW. **2007**. Mutations in *LACS2*, a long-chain acyl-coenzyme a synthetase, enhance susceptibility to avirulent *Pseudomonas syringae* but confer resistance to *Botrytis cinerea* in Arabidopsis. *Plant Physiology* **144**(2): 1093-1103.

Taurino M, Abelenda JA, Rio-Alvarez I, Navarro C, Vicedo B, Farmaki T, Jimenez P, Garcia-Agustin P, Lopez-Solanilla E, Prat S, et al. 2014. Jasmonate-dependent modifications of the pectin matrix during potato development function as a defense mechanism targeted by *Dickeya dadantii* virulence factors. *The Plant Journal* **77**(3): 418-429.

Terras FR, Eggermont K, Kovaleva V, Raikhel NV, Osborn RW, Kester A, Rees SB, Torrekens S, Van Leuven F, Vanderleyden J, et al. 1995. Small cysteine-rich antifungal proteins from radish: their role in host defense. *The Plant Cell* **7**(5): 573-588.

Terras FR, Torrekens S, Van Leuven F, Osborn RW, Vanderleyden J, Cammue BP, Broekaert WF. 1993. A new family of basic cysteine-rich plant antifungal proteins from Brassicaceae species. *Federation of European Biochemical Societies Letters* **316**(3): 233-240.

Tesfaye M, Silverstein KA, Nallu S, Wang L, Botanga CJ, Gomez SK, Costa LM, Harrison MJ, Samac DA, Glazebrook J, et al. 2013. Spatio-temporal expression patterns of *Arabidopsis thaliana* and *Medicago truncatula* defensin-like genes. *Public Library of Science One* **8**(3): e58992.

Thevissen K, de Mello Tavares P, Xu D, Blankenship J, Vandenbosch D, Idkowiak-Baldys J, Govaert G, Bink A, Rozental S, de Groot PW, et al. 2012. The plant defensin RsAFP2 induces cell wall stress, septin mislocalization and accumulation of ceramides in *Candida albicans*. *Molecular Microbiology* **84**(1): 166-180.

Thevissen K, Francois IE, Takemoto JY, Ferket KK, Meert EM, Cammue BP. 2003. DmAMP1, an antifungal plant defensin from dahlia (*Dahlia merckii*), interacts with sphingolipids from *Saccharomyces cerevisiae*. *Federation of European Microbiological Societies Microbiology Letters* **226**(1): 169-173.

Thevissen K, Warnecke DC, Francois IE, Leipelt M, Heinz E, Ott C, Zahringer U, Thomma BP, Ferket KK, Cammue BP. 2004. Defensins from insects and plants interact with fungal glucosylceramides. *Journal of Biological Chemistry* **279**(6): 3900-3905.

van de Mortel JE, Aarts MG. 2006. Comparative transcriptomics - model species lead the way. *New Phytologist* **170**(2): 199-201.

van de Mortel JE, Almar Villanueva L, Schat H, Kwekkeboom J, Coughlan S, Moerland PD, Ver Loren van Themaat E, Koornneef M, Aarts MG. 2006. Large expression differences in genes for iron and zinc homeostasis, stress response, and lignin biosynthesis distinguish roots of *Arabidopsis thaliana* and the related metal hyperaccumulator *Thlaspi caerulescens*. *Plant Physiology* **142**(3): 1127-1147.

Van der Weerden NL, Anderson MA. 2013. Plant defensins: Common fold, multiple functions. *Fungal Biology Reviews* **26**(4): 121-131.

Vandesompele J, De Preter K, Pattyn F, Poppe B, Van Roy N, De Paepe A, Speleman F. 2002. Accurate normalization of real-time quantitative RT-PCR data by geometric averaging of multiple internal control genes. *Genome biology* **3**(7): research0034.0031.

Vasseur F, Violle C, Enquist BJ, Granier C, Vile D. 2012. A common genetic basis to the origin of the leaf economics spectrum and metabolic scaling allometry. *Ecology Letters* **15**(10): 1149-1157.

Veillet F, Gaillard C, Lemonnier P, Coutos-Thevenot P, La Camera S. 2017. The molecular dialogue between *Arabidopsis thaliana* and the necrotrophic fungus *Botrytis cinerea* leads to major changes in host carbon metabolism. *Sci Rep* **7**(1): 17121.

Verbruggen N, Hermans C, Schat H. 2009. Molecular mechanisms of metal hyperaccumulation in plants. *New Phytologist* **181**(4): 759-776.

Vriens K, Peigneur S, De Coninck B, Tytgat J, Cammue BP, Thevissen K. **2016**. The antifungal plant defensin AtPDF2.3 from *Arabidopsis thaliana* blocks potassium channels. *Scientific Reports* **6**: 32121.

Wang M, Herrmann CJ, Simonovic M, Szklarczyk D, von Mering C. **2015**. Version 4.0 of PaxDb: Protein abundance data, integrated across model organisms, tissues, and cell-lines. *Proteomics* **15**(18): 3163-3168.

Weber M, Harada E, Vess C, Roepenack-Lahaye E, Clemens S. **2004**. Comparative microarray analysis of *Arabidopsis thaliana* and *Arabidopsis halleri* roots identifies nicotianamine synthase, a ZIP transporter and other genes as potential metal hyperaccumulation factors. *The Plant Journal* **37**(2): 269-281.

Wei H, Movahedi A, Xu C, Sun W, Wang P, Li D, Yin T, Zhuge Q. **2020**. Characterization, Expression Profiling, and Functional Analysis of *PtDef*, a Defensin-Encoding Gene From *Populus trichocarpa*. *Frontiers in Microbiology* **11**: 106.

Wilmes M, Cammue BP, Sahl HG, Thevissen K. **2011**. Antibiotic activities of host defense peptides: more to it than lipid bilayer perturbation. *Natural Product Reports* **28**(8): 1350-1358.

Wu Z, Liu D, Yue N, Song H, Luo J, Zhang Z. **2021**. PDF1.5 Enhances Adaptation to Low Nitrogen Levels and Cadmium Stress. *International Journal of Molecular Sciences* **22**(19).

Xu W, Dubos C, Lepiniec L. **2015**. Transcriptional control of flavonoid biosynthesis by MYB-bHLH-WDR complexes. *Trends Plant Sci* **20**(3): 176-185.

Xu Z, Mahmood K, Rothstein SJ. **2017**. ROS induces anthocyanin production *via* late biosynthetic genes and anthocyanin deficiency confers the hypersensitivity to ROS-generating stresses in Arabidopsis. *Plant & Cell Physiology* **58**(8): 1364-1377.

Xu Z, Rothstein SJ. **2018**. ROS-Induced anthocyanin production provides feedback protection by scavenging ROS and maintaining photosynthetic capacity in Arabidopsis. *Plant Signaling & Behavior* **13**(3): e1451708.

Yamaguchi-Shinozaki K, Shinozaki K. **2006**. Transcriptional regulatory networks in cellular responses and tolerance to dehydration and cold stresses. *Annual Review in Plant Biology* **57**: 781-803.

Yan J, Zhang C, Gu M, Bai Z, Zhang W, Qi T, Cheng Z, Peng W, Luo H, Nan F, et al. 2009. The Arabidopsis CORONATINE INSENSITIVE1 protein is a jasmonate receptor. *The Plant Cell* **21**(8): 2220-2236.

Yao J, Luo JS, Xiao Y, Zhang Z. **2019**. The plant defensin gene *AtPDF2.1* mediates ammonium metabolism by regulating glutamine synthetase activity in Arabidopsis thaliana. *BioMed Central Plant Biology* **19**(1): 557.

Yount NY, Yeaman MR. **2004**. Multidimensional signatures in antimicrobial peptides. *Proceedings of the National Academy of Sciences U S A* **101**(19): 7363-7368.

Yount NY, Yeaman MR. **2006**. Structural congruence among membrane-active host defense polypeptides of diverse phylogeny. *Biochimica et Biophysica Acta* **1758**(9): 1373-1386.

Zhang H, Zhao Y, Zhu J-K. **2020**. Thriving under Stress: How Plants Balance Growth and the Stress Response. *Developmental Cell* **55**(5): 529-543.

Zhang W, Zhao F, Jiang L, Chen C, Wu L, Liu Z. 2018. Different Pathogen Defense Strategies in Arabidopsis: More than Pathogen Recognition. *Cells* **7**(12): 252.

Zimmerli L, Metraux JP, Mauch-Mani B. **2001**. beta-Aminobutyric acid-induced protection of Arabidopsis against the necrotrophic fungus *Botrytis cinerea*. *Plant Physiology* **126**(2): 517-523.

Zimmerli L, Stein M, Lipka V, Schulze-Lefert P, Somerville S. **2004**. Host and non-host pathogens elicit different jasmonate/ethylene responses in Arabidopsis. *The Plant Journal* **40**(5): 633-646.

Ziv C, Zhao Z, Gao YG, Xia Y. **2018**. Multifunctional Roles of Plant Cuticle During Plant-Pathogen Interactions. *Frontiers in Plant Science* **9**: 1088.

Figure Legends

Figure 1. Localisation of the different amiRNA sequences targeting *AtPDF1.1*, *1.2a*, *1.2b*, *1.2c*, and *1.3* transcripts simultaneously and resulting in a specific decrease of transcript and protein accumulation.

(A) Alignment of seven *AtPDF1* cDNA sequences retrieved from The Arabidopsis Information Resource (TAIR; http://arabidopsis.org/index.jsp) according to the ID given in parentheses: *AtPDF1.1* (NM_106233), *AtPDF1.2a* (NM_123809), *AtPDF1.2b* (NM_128161), *AtPDF1.2c* (NM_123810), *AtPDF1.3* (NM_128160), *AtPDF1.4* (NM_101817) and *AtPDF1.5* (NM_104375). Sequences were aligned with MUSCLE 3.8.31 software (Edgar, 2004) and visualised with BOXSHADE 3.21 software (http://www.ch.embnet.org/software/BOX_form.html). The alignment of the three designed artificial microRNAs (light purple, C1; light yellow, C2; light blue, C3) are positioned on the multiple alignments. The mismatch points according to (Ossowski *et al.*, 2008) are highlighted in pink. The start and stop codons are highlighted in green (with red letters). **(B)** *AtPDF1* transcript in seedlings of the WT accession Col-0 (*n* = 12 pools of *ca*. 20 seedlings) and amiRNA lines (*n* = 24 pools of *ca*. 25 seedlings from 24 independent homozygous lines) grown under controlled *in vitro* conditions. Symbols correspond to the geometric means of relative expression obtained with three different reference genes (*ACT2 and ACT8*, *YSL8* and *EF1alpha*). Values were obtained from four independent experiments with n = 4 (WT) to n = 9 (amiRNA) replicates each (see also Supplementary Fig. S5). Error bars, lower and upper Gaussian 95% CIs. Please note that the *AtPDF1.2b* and *AtPDF1.2c* transcripts were not detected in any genotype. **(C)** Alignment of seven AtPDF1 mature peptide sequences retrieved from The Arabidopsis Information Resource (TAIR; http://arabidopsis.org/index.jsp) according to the UniProtKB ID given in parentheses: AtPDF1.1 (P30224), AtPDF1.2a (P30224), AtPDF1.2b (O80994), AtPDF1.2c (Q9FI22), AtPDF1.3 (O80995), AtPDF1.4 (P82787) and AtPDF1.5 (Q9FZ31). Sequences were aligned with MUSCLE 3.8.31 software (Edgar, 2004) and visualised with Sequence Manipulation Suite (https://www.bioinformatics.org/sms2/color_align_prop.html). Amino acid backgrounds are coloured for their identity or similarity according to their properties: non polar aliphatic (grey), aromatic (orange), unique C (yellow) and P (pink), polar uncharged (green), positively charged (red), negatively charged (blue). Peptides generated following trypsin digestion that were observed in this study are indicated within boxes differentially coloured according to their detection specificity. **(D)** Normalized intensities of detected proteins in fractionated proteome of WT, amiRNA-C2 and amiRNA-C3 lines. (**a**) NQCINLEGAK representative peptide of the AtPDF1.2a, 1.2b, 1.2c and 1.3 proteins as detected in 21 days-old seedlings (**b**) protein intensity based on NQCINLEK, LCERPSGTWSGVCGNSNACK and HGSCNYVFPAHK specific AtPDF1.1 peptides detected in dry seeds. For each experiment, three independent samples for each of the WT, amiRNA-C2 and amiRNA-C3 lines were analysed: *n* = 3 pools of *ca*. 10 seedlings **(a)** and *n* = 3 pools of *ca*. 20 mg of dry seeds **(b)**. Error bars show ± SD. Means within each genotype with the same letter are not significantly different according to one-way ANOVA followed by post hoc Tukey test, P < 0.05 . n.d: not detected.

Figure 2. Phenotypic and molecular characterisation of amiRNA plant tolerance to *B. cinerea* infection.

(A) Representative pictures of leaf symptoms five days after *B. cinerea* inoculation of *A. thaliana* leaves of WT plants and of representative homozygous lines (L) of the three amiRNA constructs (amiRNA-C1, amiRNA-C2 and amiRNA-C3) (Supplementary Dataset S1). **(B)** Lesion diameters (mean ± sem) obtained from five independent experiments (Supplementary Dataset S1) performed on WT

(white bars; *n* = 48-58) and on amiRNA-C1 (dark grey bar; *n* = 48-58), amiRNA-C2 (grey bar; *n* = 24-112) and amiRNA-C3 (light grey bar; *n* = 48-58) lines. Different letters represent significant differences between genotypes at *P* < 0.05 (Student *t*-test). **(C)** Quantification of *AtPDF1* transcript in the leaves (*n* = 5 per genotype and per treatment) of WT and amiRNA plants harvested 18 h after *B. cinerea* inoculation or mock treatment. Transcript quantification was expressed as the geometric means of relative expression obtained with three different reference genes (*ACT2 and ACT8*, *YSL8* and *expressed gene* in AT4G26410). Small symbols, means of individual samples for each *AtPDF1*. Large symbols, mean relative expression levels. Error bars, 95% CIs of five biological replicates and two triplicate qRT-PCR experiments for each genotype (see also Supplementary Fig. S9). Please note that *AtPDF1.5* transcripts were not detected in any genotype, nor in any treatment, and that in any treatment, *AtPDF1.2c* trancripts were barely detected in the amiRNA lines (*n* = 5 out of 30 samples).

Figure 3. Phenotypic characteristics of amiRNA plant tolerance to *H. arabidopsidis* NOCO2 and to *P. synringae* pv *maculicola* infection.

Representative photographs of leaf symptoms. **(A)** *H. arabidopsidis* sporulation was observed seven days after inoculation, and **(C)** leaf wilting (red spots) was observed two days after *P. synringae* pv *maculicola* ES4326 infiltration. **(B)** Number of spores *per* mg fresh weight (mean ± sem) measured seven days after *H. arabidopsidis* infection (n = 4 independent experiments; Supplementary Dataset S1) of Col-0 WT (white bar) and amiRNA-C1, C2 and C3 lines (grey bars) . **(D)** Mean (± sem) cfu count *per* cm^2 of leaf tissue of Col-0 WT (white bars) and amiRNA lines (grey bars) following infection with *P. synringae* pv *maculicola* at t = 0 and t = 2 dpi (hatched and plain bars, respectively; n = 5 independent experiments). Different letters in **(B)** and **(D)** represent significant differences between genotypes at *P* < 0.05 (Student *t*-test).

Figure 4. Increase of the dry mass of amiRNA lines in response to zinc exposure without modification of zinc accumulation

(A) Dry mass response to Zn treatment of plants cultivated in soil in two independent experiments (Supplementary Dataset S1). Whole-rosette dry mass of WT (white bars) and amiRNA lines (grey bars) measured on plants aged 54-61 days and irrigated with water (WT, *n* = 18; amiRNA-C2, *n* = 9; amiRNA-C3, *n* = 24), or with a solution of $ZnSO_4$ (WT, *n* = 12; amiRNA-C2, *n* = 9; amiRNA-C3, *n* = 24). Bars, average percent change in dry mass in response to Zn relative to the control; error bars, 95% CIs. Different letters represent significant differences between genotypes at *P* < 0.05. **(B)** Dry mass of plants grown in hydroponic conditions following 80 µM zinc treatment (n = 5 independent experiments; Supplementary Dataset S1). Dry mass was measured on whole rosettes of WT plants (circles) and amiRNA-C2 and amiRNA-C3 lines (triangles) aged 38 to 42 days and harvested 10 to 17 days after the beginning of Zn exposure (WT, *n* = 3-12; amiRNA, *n* = 3-10). Large symbols, average percent change in dry mass in response to Zn relative to the control; error bars, 95% CIs. Small symbols, individual samplings. **(C)** Zinc content of rosette leaves in the control and zinc-treated plants grown in soil (*n* = 3) or in hydroponics (*n* = 3; Supplementary Dataset S1). Bars, average values from six independent experiments (*n* = 3-13 individual plants *per* treatment and *per* experiment (small symbols)). Error bars, 95% CIs.

Figure 5. Disturbance of the anthocyanin content in amiRNA plants submitted to Zn excess.

(A) Representative zenital pictures of the abaxial rosette surface of WT and *AtPDF1*-amiRNA lines. The plants were grown in hydroponics for 39 days after sowing and treated with a solution containing 80 μM ZnSO$_4$ (Zn) or not (Control) for 14 days. Bars = 5 cm. **(B)** Anthocyanin contents of the aboveground parts of WT (circles) and amiRNA-C3 plants (triangles) cultivated in hydroponic conditions in four independent experiments. Large symbols, means of individual measurements (small symbols) performed on plant rosettes aged 32 or 26 days after germination and treated with 80 μM ZnSO$_4$ (grey symbols) or untreated (black symbols) at the time of harvest (0 to 15 days after the start of zinc exposure). The scale is indicated in Log$_{10}$ and regression lines are indicated (r = -0.68, P = 0.011; r = -0.08, P = 0.81; r = -0.66, P = 0.014; r = -0.60, P = 0.04 for the control and Zn-treated WT and for the control and Zn-treated amiRNA line, respectively; n = 2-4 individual plants *per* treatment, *per* experiment and time point).

Figure 6. Cuticle permeability is affected in amiRNA plants, and zinc excess causes a similar dry mass decrease in the WT and the cuticle mutant plants.

(A) Cuticle permeability assay with toluidine blue. Representative photographs of three independent experiments conducted on different genotypes (see Supplementary Dataset S1). **(B)** Response to Zn excess of the shoot dry mass of different *A. thaliana* genotypes cultivated in hydroponics. Dry mass was measured 33 days after sowing in two independent experiments (Exp. 1, Exp. 2) on *A. thaliana* plants treated with a control solution or a solution containing 80 μM ZnSO$_4$ for 11 days. WT plants (n = 15, 15 and n = 36, 43); amiRNA-C2 (n = 35, 9 and n = 0 in Exp. 2), amiRNA-C3 (n = 6, 7 and n = 17, 21) and *lacs2-3* (n = 9, 18 and n = 14, 19) mutant. Within each experiment, bars represent the average percent change in dry mass in response to zinc relative to the control, and error bars represent 95% CIs. Different letters indicate significant differences of computed CIs within each experiment. ND, not determined.
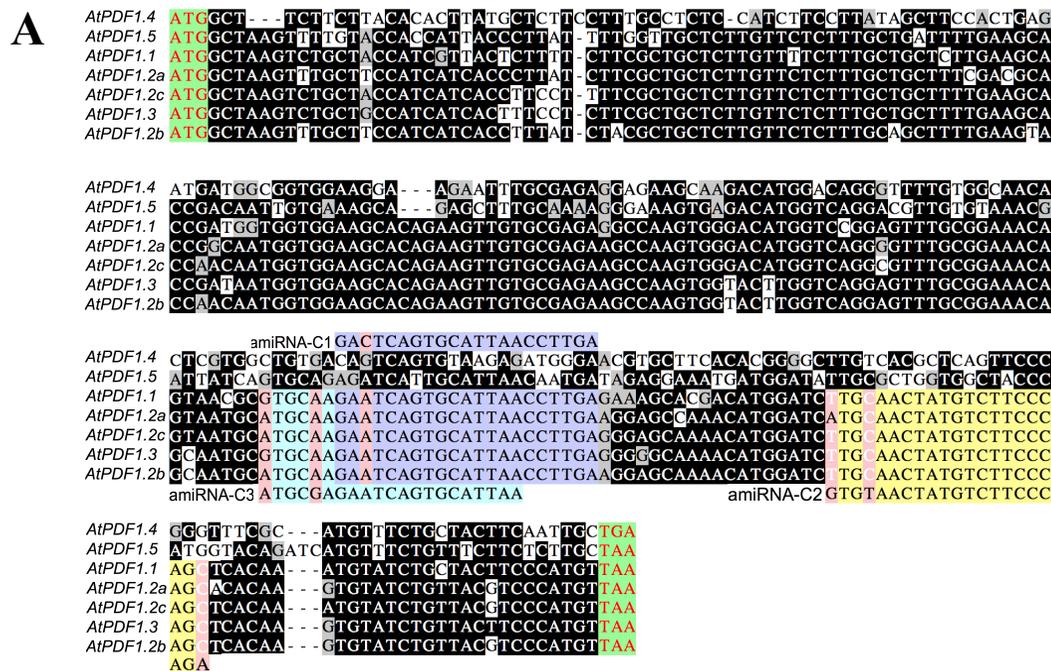
Figure 1

Figure 2

FIGURE 3

FIGURE 4

FIGURE 5

A FIGURE 6

WT
amiRNA-C1L8
amiRNA-C1L2
amiRNA-C2L2
amiRNA-C2L16
amiRNA-C3L1
amiRNA-C3L4
Atpdf1.4-Atpdf1.5
lacs2.3

B

Exp. 1 — Exp. 2

Dry mass response to Zn (%)

WT, amiRNA-C2 (ND), amiRNA-C3, *lacs2-3*